**Paleornithological Research 2013**

Proceed. 8th Internat. Meeting Society of Avian Paleontology and Evolution

Ursula B. Göhlich & Andreas Kroh (Eds)

naturhistorisches museum wien

# Ontogenetic change of morphology and surface texture of long bones in the Gray Heron (*Ardea cinerea*, Ardeidae)

JUNYA WATANABE & HIROSHIGE MATSUOKA

*Department of Geology and Mineralogy, Kyoto University, Kyoto, Japan;*
*E-mail: watanabe-j@kueps.kyoto-u.ac.jp*

**Abstract** — Although the importance of assessing ontogenetic age or developmental stage of fossil materials is widely recognized, information on avian postnatal skeletal ontogeny, which forms a basis for ageing criteria for bird fossils, is seriously lacking. One potentially useful ontogenetic ageing method in avian paleontology is textural ageing, in which surface textures of long bones are examined to assess developmental stage. To date, ontogenetic change of surface textures in long bones has been intensively described in only one species, the Canada Goose (*Branta canadensis*). In this study, through original preparation and examination of an ontogenetic series of specimens, which consists of 13 chicks (including one fledgling), two juveniles (birds under one-year-old) and two adults, postnatal ontogenetic changes of macroscopic morphology and surface texture of six major long bones (humerus, ulna, carpometacarpus, femur, tibiotarsus and tarsometatarsus) of the Gray Heron (*Ardea cinerea*, Ardeidae) are described and illustrated. Most long bones continue to grow in length until reaching their adult size range around the time of fledging. Epiphyses are generally not ossified before fledging; in both ends of femur and proximal end of tibiotarsus, distinct ossification centers can be observed. Generally, long bones of chicks are characterized by rough surface textures, including striated structures near epiphyses and fibrous/porous surface with frequent penetrating pits in the midshaft. Long bones of juveniles are characterized by faint grooves and/or dimples, but rough striated structure may remain in the proximal regions of tibiotarsus and tarsometatarsus. In adults smooth surface pattern dominates. Inter-elemental variation in surface texture in one species is likely to represent taxon-specific patterns of relative timings of maturity among long bones, which would be related to various aspects of skeletal ontogeny in birds. At this time, textural ageing on birds with interrupted growth might be somewhat problematic because of a lack of sufficient data.

**Key words:** bone growth, textural ageing, epiphysis, Ardeidae

## Introduction

Assessing ontogenetic age or developmental stage (ontogenetic ageing) of fossil materials is an essential and crucial step in most paleontological investigations, including taxonomical, paleoecological, faunistic, and evolutionary studies. Incorrect ontogenetic ageing will easily lead to taxonomical confusion or other misled conclusions in such studies. In avian paleontology, except for very rare cases, fossil remains are almost always skeletal elements, which are often isolated and damaged. Among them, long bones are of particular importance for their relative abundance as fossil remains and ease of identification. Reliable ontogenetic ageing criteria for (isolated) avian long bones are desired. As a basis for such criteria, precise and detailed understanding of the ontogeny of avian long bones is necessary.

Although embryological development of the avian skeleton has been intensively investigated


published 10 Dec. 2013

(*e.g.*, Fujioka 1955; Rogulska 1962; Starck 1993), there have been relatively few studies investigating postnatal ontogeny. Examples of previous studies which investigated postnatal ontogeny of avian skeletons include those focusing on metrical aspects (*e.g.*, Marples 1930; Klíma 1965; Cane 1993; Hayward *et al.* 2009; Picasso 2012), histological aspects (*e.g.*, Starck & Chinsamy 2002; de Margerie *et al.* 2004) and mechanical/functional aspects (*e.g.*, Bjordal 1987; Carrier & Leon 1990; Dial & Carrier 2012). However, there have been very few studies focusing on macroscopic morphological aspects of the avian skeleton in postnatal ontogeny, which would be useful for establishing ontogenetic ageing criteria for bird fossils. Previous studies that gave partial descriptions or illustrations on macroscopic morphology in avian postnatal skeletal ontogeny include; Huggins *et al.* (1942), who described and illustrated stained skeletons of the growing House Wren (*Troglodytes aedon aedon*); Beale (1985, 1991), who investigated ontogeny of long bones of a growing kiwi (*Apteryx australis mantelli*) through ten years of radiological study; and Picasso (2012), who studied ontogenetic allometry in the hindlimb skeleton of the Greater Rhea (*Rhea americana*) and figured hindlimb long bones at various ages. To form a basis for ontogenetic ageing criteria for bird fossils and for other morphological studies, it is desirable to accumulate data on skeletal ontogeny of various avian taxa with comprehensive descriptions and illustrations.

As a practice in many previous avian paleontological and zooarchaeological studies, "incompletely ossified" skeletal materials were considered to represent immature or juvenile individuals, often without firm justification (*e.g.*, Howard 1929). Degrees of ossification in skeletal specimens of immature individuals have been sporadically described or illustrated by some authors for comparative purpose (Callison & Quimby 1984; Sanz *et al.* 1997; Serjeantson 2002). Recently, Tumarkin-Deratzian *et al.* (2006) gave a comprehensive review on this topic and evaluated surface texture of the humerus, femur and tibiotarsus as an ontogenetic indicator in the Canada Goose (*Branta canadensis*). They examined over 80 skeletal specimens of the species, described the relationship between surface textures of long bones and developmental stages, as well as their underlying histological features, and formed a basis for a practical ontogenetic ageing criterion. Given the fact that birds have diverse ontogenetic strategies (*e.g.*, precocial-altricial spectrum; Starck & Ricklefs 1998), further studies are needed to test the presence or nature of taxon-specific variation.

In this study, to form a basis for ontogenetic ageing criteria for bird fossils, a postnatal ontogenetic series of skeletal specimens of a common Recent species, the Gray Heron (*Ardea cinerea* Linnaeus, 1758, Family Ardeidae), was prepared and examined. Ontogenetic changes of macroscopic morphology and surface textures of six major long bones (humerus, ulna, carpometacarpus, femur, tibiotarsus and tarsometatarsus) are described and illustrated. Some additional features of morphological interests are also described, such as epiphysial ossification centers in femur and tibiotarsus.

## Materials and Methods

**Sampled species.** In this study, an ontogenetic series of the Gray Heron (*Ardea cinerea*) was collected and prepared in order to observe ontogenetic changes of morphology and surface texture of long bones. *Ardea cinerea* is a large heron species whose adults reach 90–98 cm in length and 1020–2073 g in weight (Kushlan & Hancock 2005). Some subspecies can be recognized based on geographical variation in plumage. All individuals studied were collected in Japan, thus are from the East Asian subspecies *A. c. jouyi* Clark, 1907 (Yamashina 1941; Kushlan & Hancock 2005). Sexual variation in skeletal dimensions is generally significant but slight (about 2–4 %; Boev 1987). In the breeding season, they build colonies in the forest canopy and drop chick carcasses, facilitating collection of large samples of chicks. In Japan, eggs are laid from April to early May, and chicks hatch after 25–28 days of incubation (Yamashina 1941). Chicks are (semi-)altricial: hatchlings are fed by parents, covered by down, have open eyes and can stand within a day (Starck & Ricklefs 1998; Kushlan & Hancock 2005). They can clamber away from nests at about six weeks old, and

fledge and become capable of flight at seven to eight weeks old (Yamashina 1941). Individual developmental stages can be determined by distinctive age-related plumage (Yamashina 1941; Milstein *et al.* 1970). It is commonly thought that they breed after the second winter, but breeding by yearlings is not exceptional (Milstein *et al.* 1970; Kushlan & Hancock 2005). Thus, sexual maturity could be attained around (or perhaps before) one-year-old in this species.

In this study, three postnatal developmental stages are recognized: chick, juvenile, and adult. Note that definitions of these terms might be different from both ornithological and paleontological conventions (see below). Each individual is classified into one of the three stages based on its plumage. Exact absolute age was not available for any of the individuals, so they are ordered in a presumed ontogenetic sequence. In chick stage, individuals are ordered by increasing external measurements. Juveniles are ordered by their collection date (from earlier to later). Ordering in adults is done arbitrarily.

**Description of sample series.** The study series consists of 13 chicks, two juveniles and two adults. Each individual is labeled with a prefix ("C" for chicks, "J" for juveniles and "A" for adults), and a number to represent its place in the ontogenetic sequence defined above (*i.e.*, C1, C2,..., C13, J14, J15, A16 and A17). All individuals were collected in and around Kyoto, Japan, so the geographical variation within the series is considered to be minimal. Sexes of most individuals could not be determined, so both sexes were pooled to form a single series. Definitions and descriptions of three developmental stages are given below. Date of death and external measurements of each individual are summarized in Tab. 1. The study series is stored at the Department of Geology and Mineralogy, Kyoto University, Kyoto, Japan. See Tab. 1 for repository numbers of the specimens.

*Chick* — This stage refers to birds after hatching and before leaving the colony. Birds of this stage are typically characterized by functionally immature plumage, including sheathed flight feathers. All chick individuals included in the study series were found dead at a breeding colony in Kyoto, Japan. A total of 23 chicks were

**TABLE 1.** List of the individuals included in the study series. Linear measurements (in mm), body weight (in grams), and collection date (year. month. day) are given. Body length is measured from the bill tip to the tip of the tail with the back on a flat plane and the neck extended. Asterisks indicate underestimated values due to damage on carcasses.

| Individual code | Repository number | Collection date | Body length | Body weight | Culmen length | Tarsus length |
|---|---|---|---|---|---|---|
| C1 | RAJ-1 | 2009.06.07 | 401 | 488 | 51 | 68 |
| C2 | RAJ-2 | 2010.04.21 | 417* | 470* | 50 | 77 |
| C3 | RAJ-3 | 2009.05.19 | 456* | 520* | 61 | 78 |
| C4 | RAJ-4 | 2010.06.02 | 462* | 820* | 60 | 90 |
| C5 | RAJ-5 | 2011.06.13 | 474* | 700* | 61 | 91 |
| C6 | RAJ-6 | 2010.04.29 | 495* | 840* | 62 | 93 |
| C7 | RAJ-7 | 2009.05.27 | 484* | 682* | 65 | 91 |
| C8 | RAJ-8 | 2009.05.22 | 530* | 782* | 69 | 99 |
| C9 | RAJ-9 | 2011.05.31 | 530* | 940* | 70 | 102 |
| C10 | RAJ-10 | 2009.05.24 | 564* | 835* | 74 | 109 |
| C11 | RAJ-11 | 2009.05.24 | 576* | 790* | 80 | 112 |
| C12 | RAJ-12 | 2009.05.19 | 552* | 940* | 80 | 132 |
| C13 | RAJ-13 | 2009.06.07 | 886 | 1362 | 100 | 146 |
| J14 | RA-1002 | 1995.06.18 | 980 | 1220 | 118 | 171 |
| J15 | RAJ-27 | 1999.08.02 | 960 | 1180 | 115 | 162 |
| A16 | RAJ-28 | 2012.03.15 | 910* | 1600* | 127 | 168 |
| A17 | RA-1001 | (not recorded) | 940 | 1050* | 112 | 145 |

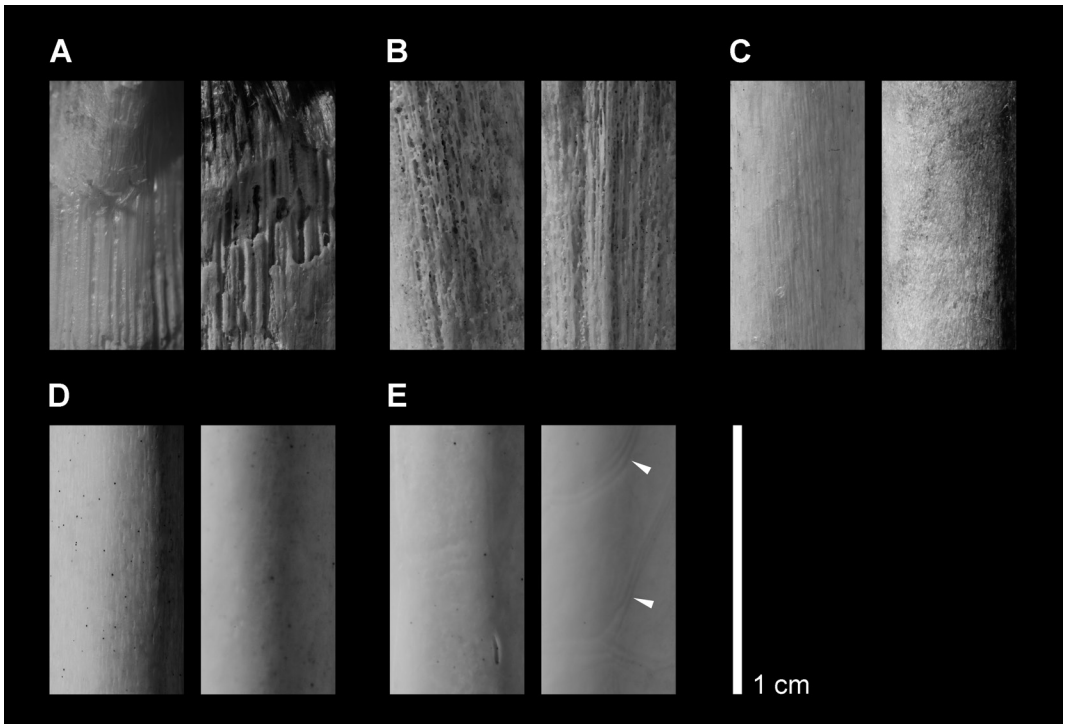


**FIGURE 1.** Examples of surface textural patterns. **A**) pattern A: left, proximal tibiotarsus in C5, cranial view, showing striated pattern running longitudinally with few transverse struts; right, damaged surface of proximal tibiotarsus in C8, medial view, showing low bone density underlying this pattern. **B**) pattern B: left, proximal humerus in C11, ventral view, showing striated structure with frequent transverse struts; right, proximal tarsometatarsus in C11, cranial view. **C**) pattern C: left, midshaft of humerus in C11, cranial view, showing fibrous structure with shallow grooves; right, midshaft of femur in C11, caudal view, showing densely distributed dimples. **D**) pattern D: left, midshaft of humerus in J14, caudal view, surface showing short longitudinal grooves and dimples; right, midshaft of ulna in J14, dorsal view, showing shallowly dimpled surface. **E**) pattern E: midshaft of humerus in A17, ventral view, with a nutrient foramen on right bottom; right, distal tibiotarsus in A17, caudal view, with vascular grooves (white arrowheads). Upper side of each photograph is proximal side of the long bone.

obtained, and 13 of them had a nearly complete set of long bones and thus were included in the study series. The largest chick studied (C13) had both an almost complete plumage including flight feathers and remains of natal down at the tip of the crest. Thus it is considered to represent the fledgling period, or seven to eight weeks old (Yamashina 1941; Milstein *et al.* 1970). All others (C1–C12) had not yet fledged, so they are considered to be younger than C13.

*Juvenile* — This stage includes birds having left the colony and are under one year old. Juveniles are readily distinguishable from adults by their distinct plumage, including gray forehead and neck and less developed crown. Yearlings, or one-year-old birds, have a similar plumage, but they can be distinguished by several distinctive features, including the color pattern of the bill (Milstein *et al.* 1970). Two juveniles were included in the study series, both of which were collected around Kyoto in their first summer (thus are considered to be about two to four months old).

*Adult* — In this study, this stage refers to all birds after attaining the second year external coloration (*i.e.*, one-year-old and older). Although further distinction (*e.g.* yearlings, subadults and adults) within this stage is possible based on plumage, this was not attempted because the sample size was too small to allow meaningful comparison. Two adults, collected around Kyoto, were included in the study series.

**Preparation of specimens.** All collected individuals were temporarily stored frozen until preparation. After thawing, left long bones (humerus, ulna, carpometacarpus, femur, tibiotarsus [+ fibula] and tarsometatarsus) were

isolated from the carcasses by dissection, and the surrounding soft tissue was carefully removed from the bones. Isolated bones were soaked in dilute solution of hydrogen peroxide (ca. 2 %) until they were bleached (usually after 12–24 hours). After bleaching, they were further cleaned manually and then dried. This procedure deforms cartilages on epiphysial area of long bones from their original shape, but it makes them translucent to a certain degree, which allows ossification centers to be observed. The rest of the body was refrozen for future studies.

**Classification of surface textures.** Surface textures of long bones, which have been suggested to be an useful ontogenetic indicator in the Canada Goose (*Branta canadensis*) by Tumarkin-Deratzian *et al.* (2006), are described and figured in the study series. They show considerable variation among individuals and elements, and even within a single element (see below for detail). For comparisons among individuals and elements, various surface textures are classified into the five patterns described below. These patterns are applied to surface texture in certain area on a bone, rather than to the texture of an entire bone, unlike the "texture types" in Tumarkin-Deratzian *et al.* (2006). Examples of surface patterns are shown in Fig. 1.

Variation of textural patterns in a single element is most prominent in its longitudinal direction; longitudinally, one bone show up to four texture patterns at one transverse position of its shaft, whereas transversely (or circumferentially), one bone show no more than two patterns at one longitudinal position of its shaft. Thus one-dimensional longitudinal distribution of textural patterns in a long bone can be used as a representation of overall distribution of patterns in that bone. In practice, the dominant textural pattern at one longitudinal position is regarded as the representing pattern at that position; the dominant pattern here refers to that the pattern is more widely distributed transversely than any other patterns, without concerning articular surfaces and apparent muscular/ligamental attachment sites. Longitudinal distribution of one pattern is defined as the length of longitudinal section where the pattern is dominant, and is measured between the two points at which the pattern occupies 50 % of transverse circumference of the shaft (measured with a tape measure rolled on the shaft). This simplified one-dimensional distribution is used for graphical presentation and comparison among elements and individuals.

*Pattern A* (Fig. 1A) — This pattern is defined as a striated structure with smooth surface and few transverse struts. Typically, it shows loose structure formed by relatively thick longitudinal ridges and shallow furrows without transverse struts. This pattern is always accompanied by epiphysial cartilages on one side. When seen from the epiphysis, it shows a rather porous appearance.

*Pattern B* (Fig. 1B) — This pattern is defined as a striated structure with rough surface and frequent transverse struts. This pattern shows the roughest appearance among the five, and is composed of thin ridges, or trabeculae, deep grooves running longitudinally and with frequent transverse struts.

*Pattern C* (Fig. 1C) — This pattern is defined by the absence of structures characterizing the above patterns, and the frequent presence of shallow longitudinal grooves and/or dimples, which occasionally form penetrating pits on the bone wall. When present, grooves often reach five millimeters or more in length. This pattern gives a fibrous/porous and non-glossy appearance.

*Pattern D* (Fig. 1D) — This pattern is defined by the absence of apparent striated patterns and penetrating pits, and the presence of faint longitudinal grooves and/or dimples. Typically, grooves and dimples are less densely distributed, and length of grooves are smaller (several millimeters at maximum) than in pattern C. This pattern gives an overall glossy appearance, but grooves and dimples can easily be observed with a hand lens.

*Pattern E* (Fig. 1E) — This pattern is defined by the absence of striated structure, penetrating pits, and grooves/dimples (except at the attachment sites of muscles, ligaments or articular capsules). Occasional traces of vascular canals can be observed on this pattern. This pattern gives an overall glossy and smooth appearance.

**Terminology and measurements.** Osteological terminology follows that of Baumel & Witmer (1993). The term "epiphysis" as used here


**FIGURE 2.** Ontogenetic morphological change of the humerus in *Ardea cinerea*. From left to right, C1, C2, C5, C8, C9, C11, C12, C13, J14, J15, A16 and A17.

refers to either end of a long bone, not specifically to independent ossification centers; the latter is called "epiphysial ossification center" to avoid confusion. But the term "diaphysis" of a long bone is used to refer either to the primary ossification center of the shaft, or to the shaft in general. Dimensions of long bones were measured after drying, thus they might underestimate actual values in incompletely ossified bones; such underestimated values are marked in the table of measurements (Tab. 2). The dimension "ossified length" was measured in incompletely ossified bones and refers to the approximate length of ossified diaphysis and fused epiphysial ossification centers, if applicable. In wing bones (humerus, ulna, and carpometacarpus), "width" refers to dorsoventral width and "depth" refers to craniocaudal depth; whereas in leg bones (femur, tibiotarsus, and tarsometatarsus), "width" refers to mediolateral width and "depth" refers to craniocaudal depth. In humeri, greatest and smallest diameters of the shaft at the midpoint are presented, which are slightly diagonal to the width and depth, respectively, of the shaft. In tibiotarsi, length of the bone is measured from the proximal articular surface, rather than from the cnemial crest, to the distal condyles. Measurements on skeletal elements were performed with a digital caliper (Mitutoyo Corp., Japan; precision = ± 0.02 mm) to the nearest tenth millimeter.

## Description of morphology

Overall morphology of long bones in *Ardea cinerea* show considerable ontogenetic change from chick through juvenile to adult stage. Detailed morphological description, with emphasis on ontogenetic variable characters, are given below. Long bones of selected individuals are illustrated in Figs 2–6. Details of skeletal features described are illustrated in Figs 7 and 8. Selected osteological measurements are given in Tab. 2.

**Humerus** (Figs 2, 7A, 7B). *Chick* — Overall shape of the bone is relatively uniform longitudinally, with less developed osteological features on both ends. Caput humeri, Tuberculum ventrale, Incisura capitis, Tuberculum dorsale, and Sulcus transversus are all cartilaginous in C1–C12. In C13, they are all present, but Caput humeri is less developed than in juveniles and adults, with porous surface and flat proximal margin. Impressio coracobrachialis and Linea m. latissimi dorsi are observable only in C13. Crista deltopectoralis is almost absent in C1–C7, present as a blunt projection with slightly convex dorsal surface in C8–C12, and developed with concave dorsal sur-


**FIGURE 3.** Ontogenetic morphological change of the ulna in *Ardea cinerea*. From left to right, C1, C2, C5, C8, C9, C11, C12, C13, J14, J15, A16 and A17.

face in C13. Foramen pneumaticum (pf in Fig. 7A) is open in the cartilaginous proximal end in C1–C12, and the surrounding area is ossified in C13; its distal margin is always extending distally to form a prominent fossa on the ossified area, which is covered by periosteum and occasional thin bone wall (Fig. 7A). Foramina nutrientia are present on Margo ventralis in the midshaft region, and single in C1–C4, C7, C8, C11, and C13, but double in C5, C6, C9, C10, and C12; they are almost always with large openings (about 3.5 × 0.7 mm, with long axis parallel to the shaft; Fig. 7B), and one of the double foramina is occasionally covered by thin bone wall. Condyli dorsalis et ventralis are cartilaginous in C1–C12, ossified but with porous surface in C13. Epicondyli dorsalis et ventralis are cartilaginous in C1–C12, ossified in C13. Proximal margin of Fossa m. brachialis is observable on ossified area, but its distal margin is indistinct.

*Juvenile* — Caput humeri is developed proximocaudally, rounded, and surrounded by numerous foramina on its margin (Fig. 7A). Tuberculum ventrale, Incisura capitis, Tuberculum dorsale, Crista deltopectoralis, and Linea m. latissimi dorsi are developed as in adults. Foramen pneumaticum (pf in Fig. 7A) is long proximodistally; its distal part is covered by periosteum (Fig. 7A) and serves as attachment for M. humerotriceps. Foramen nutriens is single in all cases, and opens on Margo ventralis at around the midpoint of the shaft with an apparently larger opening than in adults (about 4.0 × 0.4 mm, with long axis parallel to the shaft; Fig. 7B). Condyli dorsalis et ventralis are developed as in adult, but with numerous foramina on their margins. Epicondyli dorsalis et ventralis, and Fossa m. brachialis are developed as in adults.

*Adult* — Caput humeri is developed proximocaudally and rounded, with few foramina on its margin. Tuberculum ventrale, Incisura capitis, Tuberculum dorsale are all well developed. Crista deltopectoralis is well developed craniodorsally with concave dorsal surface. Linea m. latissimi dorsi is prominent. Foramen pneumaticum (pf in Fig. 7A) is just slightly longer longitudinally than dorsoventrally; its distal margin extending no more distally than the base of Crus dorsale fossae. Foramen nutriens is single in all cases, and opens on Margo ventralis at around the midpoint of the shaft, with a minute opening (about 2.0 × 0.3 mm; Fig. 7B). Condyli dorsalis

**TABLE 2.** Osteological measurements of the study series (in mm). Daggers indicate those including dried cartilaginous area (and thus underestimated values). Asterisks indicates underestimated values because of damage to bones. See Materials and Methods for notes on measurements.

| | C1 | C2 | C3 | C4 | C5 | C6 | C7 | C8 | C9 | C10 | C11 | C12 | C13 | J14 | J15 | A16 | A17 |
|---|---|---|---|---|---|---|---|---|---|---|---|---|---|---|---|---|---|
| **Humerus** | | | | | | | | | | | | | | | | | |
| length | †69.6 | †84.0 | †91.3 | †95.9 | †98.0 | †110.1 | †102.7 | †127.3 | †125.7 | †130.0 | †139.6 | †150.7 | 164.8 | 173.3 | 176.9 | 178.3 | 162.7 |
| ossified length | 61.3 | 76.9 | 82.7 | 85.9 | 89.5 | 100.6 | 93.7 | 115.8 | 120.1 | 121.9 | 129.4 | 141.0 | — | — | — | — | — |
| proximal width | †9.5 | †13.2 | †12.7 | †16.9 | †15.9 | †15.5 | †13.5 | †15.8 | †17.1 | †16.9 | †18.7 | †18.7 | 22.8 | 25.7 | 24.9 | 25.2 | 24.6 |
| greatest diameter at midpoint | 4.0 | 5.1 | 5.0 | 5.6 | 6.0 | 6.6 | 5.9 | 7.0 | 7.5 | 7.2 | 7.5 | 8.2 | 8.6 | 9.9 | 9.9 | 10.5 | 10.1 |
| smallest diameter at midpoint | 3.7 | 4.4 | 4.5 | 5.4 | 5.3 | 5.6 | 5.1 | 6.4 | 7.1 | 6.5 | 7.0 | 7.2 | 7.7 | 8.8 | 8.7 | 8.9 | 8.5 |
| distal width | †9.3 | †10.6 | †13.3 | †14.4 | †13.6 | †14.0 | †13.1 | †15.1 | †15.9 | †15.6 | †16.9 | †18.5 | 20.6 | 22.5 | 22.4 | 23.4 | 21.8 |
| **Ulna** | | | | | | | | | | | | | | | | | |
| length | †68.6 | †84.4 | †88.9 | †97.8 | †98.7 | †116.5 | †103.6 | †132.6 | †153.7 | †137.4 | †154.5 | †162.8 | 194.0 | 209.6 | 214.8 | 208.8 | 194.3 |
| ossified length | 60.0 | 71.6 | 78.0 | 82.9 | 89.8 | 105.8 | 91.8 | 118.5 | 121.7 | 124.8 | 145.3 | 155.0 | — | — | — | — | — |
| proximal width | †6.9 | †9.1 | †9.4 | †10.8 | †11.0 | †11.5 | †8.4 | †11.3 | †10.1 | †10.3 | †10.4 | †13.2 | 14.8 | 16.0 | 15.7 | 15.8 | 15.4 |
| shaft width at midpoint | 3.1 | 3.4 | 3.2 | 4.0 | 4.2 | 4.0 | 4.1 | 5.1 | 5.4 | 4.7 | 5.4 | 5.8 | 6.6 | 7.4 | 7.5 | 7.8 | 7.5 |
| shaft depth at midpoint | 2.5 | 3.3 | 2.6 | 3.2 | 3.1 | 3.2 | 3.1 | 3.9 | 4.1 | 4.0 | 4.7 | 4.6 | 5.7 | 6.0 | 6.2 | 6.3 | 6.1 |
| distal width | †4.3 | †5.3 | †4.6 | †6.2 | †6.7 | †7.4 | †5.9 | †6.7 | †8.1 | †6.1 | †7.4 | †8.2 | 10.3 | 10.1 | 11.7 | 10.5 | 10.7 |
| **Carpometacarpus** | | | | | | | | | | | | | | | | | |
| length | †35.1 | †43.6 | †45.2 | †48.2 | †50.4 | †58.7 | †52.9 | †65.3 | †67.1 | †67.4 | †75.3 | †80.2 | 87.8 | 95.0 | 97.5 | 93.7 | 85.9 |
| ossified length | 28.8 | 35.7 | 39.0 | 40.4 | 44.9 | 50.8 | 43.9 | 56.6 | 59.0 | 60.0 | 69.1 | 71.2 | — | — | — | — | — |
| width of major metacarpus | 2.7 | 2.7 | 2.7 | 3.1 | 3.2 | 3.2 | 3.3 | 3.5 | 3.8 | 3.5 | 4.0 | 4.2 | 4.6 | 5.2 | 5.6 | 5.7 | 5.1 |

**TABLE 2.** (continued)

| | C1 | C2 | C3 | C4 | C5 | C6 | C7 | C8 | C9 | C10 | C11 | C12 | C13 | J14 | J15 | A16 | A17 |
|---|---|---|---|---|---|---|---|---|---|---|---|---|---|---|---|---|---|
| **Femur** | | | | | | | | | | | | | | | | | |
| length | †62.0 | †68.9 | †73.2 | †75.4 | †75.1 | †78.1 | †75.2 | †82.2 | †84.3 | †83.2 | †79.8 | —* | 85.6 | 92.8 | 94.3 | 93.5 | 84.0 |
| ossified length | 55.1 | 61.4 | 65.1 | 66.4 | 66.9 | 71.0 | 67.1 | 75.4 | 76.2 | 76.6 | 74.5 | —* | — | — | — | — | — |
| proximal width | †8.9 | †10.4 | †12.4 | †11.2 | †11.6 | †11.6 | †10.9 | †11.8 | †11.7 | †12.0 | †12.8 | —* | 14.4 | 15.4 | 15.6 | 15.5 | 14.5 |
| shaft width at midpoint | 4.6 | 4.9 | 5.4 | 6.0 | 6.0 | 5.7 | 5.5 | 5.6 | 6.4 | 5.9 | 6.2 | —* | 5.8 | 7.5 | 6.7 | 6.8 | 7.3 |
| shaft depth at midpoint | 4.8 | 5.0 | 5.0 | 6.0 | 5.9 | 5.3 | 5.5 | 5.7 | 6.6 | 6.2 | 6.1 | —* | 6.2 | 7.0 | 6.9 | 6.9 | 6.5 |
| distal width | †10.3 | †11.2 | †12.5 | †12.2 | †12.6 | †12.3 | †12.0 | †12.1 | †13.9 | †13.5 | †14.0 | —* | 14.4 | 15.5 | 15.5 | 15.8 | 14.0 |
| **Tibiotarsus** | | | | | | | | | | | | | | | | | |
| length | †83.6 | †91.8 | †101.9 | †109.3 | †105.7 | †116.9 | †110.7 | †127.2 | †131.0 | †132.1 | †138.8 | †150.8 | 196.4 | 224.2 | 221.1 | 216.3 | 202.1 |
| ossified length | 73.5 | 80.8 | 88.9 | 92.7 | 93.9 | 103.8 | 98.9 | 113.1 | 116.2 | 116.9 | 127.6 | 143.1* | — | — | — | — | — |
| proximal width | †6.8 | †10.1 | †9.1 | †9.8 | †9.9 | †10.9 | †8.6 | †10.2 | †11.1 | †11.0 | †11.4 | —* | 12.2 | 13.4 | 12.9 | 13.6 | 12.7 |
| width below proximal end | 6.7 | 7.8 | 8.2 | 9.5 | 9.4 | 10.0 | 8.7 | 10.0 | 10.7 | 10.7 | 12.0 | 11.8 | 9.1 | 7.8 | 7.7 | 8.1 | 8.2 |
| depth below proximal end | 10.3 | 13.2 | 13.0 | 14.3 | 14.3 | 15.1 | 12.9 | 14.4 | 16.2 | 15.8 | 15.2 | 15.9 | 10.7 | 9.6 | 10.0 | 11.9 | 9.5 |
| narrowest shaft width | 4.1 | 4.1 | 4.3 | 4.9 | 4.9 | 4.4 | 4.7 | 4.7 | 5.1 | 4.8 | 5.8 | 5.9 | 5.1 | 6.0 | 6.0 | 5.9 | 5.8 |
| distal width | 9.7 | 12.2 | 11.9 | 12.8 | 12.6 | 12.9 | 12.4 | 12.5 | 13.0 | 12.0 | 12.0 | 12.5 | 12.2 | 12.8 | 13.3 | 13.6 | 12.1 |
| **Tarsometatarsus** | | | | | | | | | | | | | | | | | |
| length | †62.7 | †68.4 | †77.3 | †85.5 | †82.6 | †88.0 | †89.9 | †100.9 | †105.4 | †102.9 | †111.9 | †131.7 | 144.7 | 169.6 | 161.3 | 172.9 | 145.6 |
| ossified length | 51.6 | 56.8 | 65.0 | 73.1 | 70.8 | 75.9 | 78.4 | 89.1 | 90.1 | 93.9 | 101.1 | 119.9 | — | — | — | — | — |
| proximal width | 10.2 | 12.5 | 12.7 | 14.4 | 14.5 | 15.0 | 14.1 | 14.9 | 15.5 | 15.5 | 16.1 | 16.8 | 13.8 | 14.7 | 14.9 | 14.8 | 13.3 |
| shaft width below hypotarsus | 9.1 | 11.3 | 11.7 | 13.2 | 12.3 | 13.3 | 12.3 | 13.6 | 14.2 | 13.9 | 14.8 | 15.6 | 9.2 | 9.6 | 8.2 | 7.2 | 6.6 |
| narrowest shaft width | 5.0 | 5.3 | 4.9 | 5.5 | 5.5 | 5.3 | 5.3 | 5.0 | 5.4 | 5.5 | 5.4 | 5.6 | 5.0 | 5.4 | 5.3 | 5.6 | 5.3 |
| distal width | 11.0 | 11.1 | 11.4 | 12.0 | 12.3 | 12.1 | 12.5 | 12.8 | 13.1 | 13.1 | 13.6 | 14.0 | 13.2 | 13.9 | 14.8 | 14.3 | 13.5 |

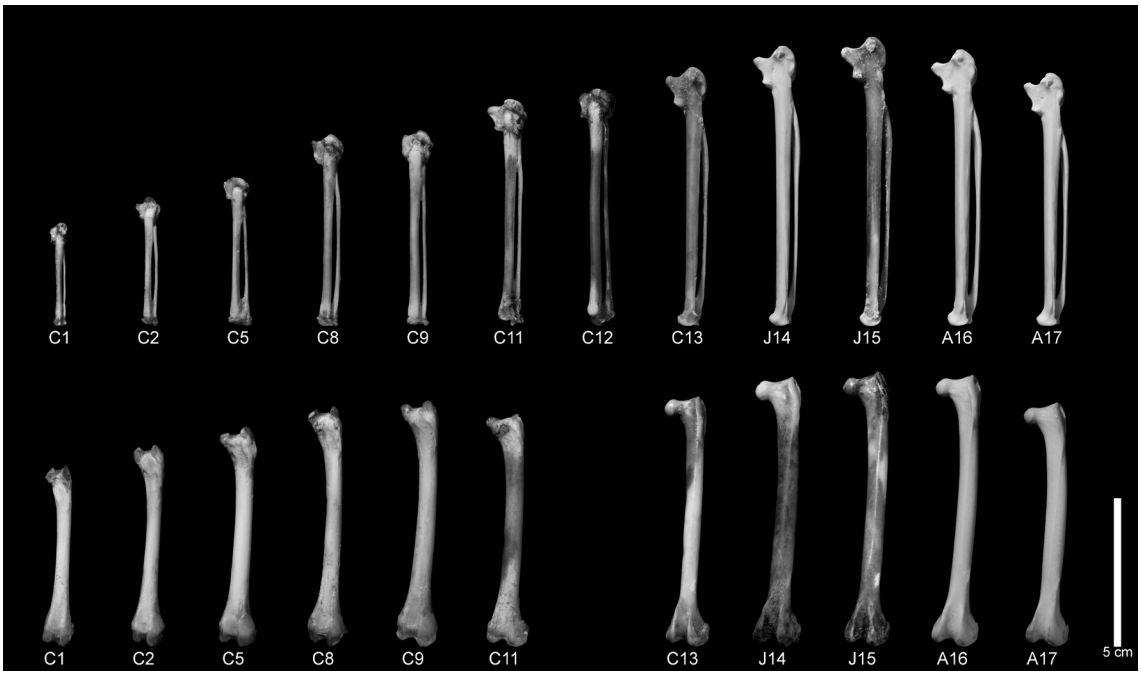


**FIGURE 4.** Ontogenetic morphological changes of the carpometacarpus (top) and femur (bottom) in *Ardea cinerea*. From left to right, C1, C2, C5, C8, C9, C11, C12 (missing for the femur), C13, J14, J15, A16 and A17 for each.

et ventralis are developed craniodistally, with few surrounding foramina. Epicondyli dorsalis et ventralis are well developed. Entire margin of Fossa m. brachialis is distinct.

**Ulna** (Fig. 3). *Chick* — Shaft curvature is less prominent in C1–C12, and slightly more weakly curved in C13 than in adults. Extremitas proximalis ulnae is cartilaginous in C1–C12, and ossified in C13 with porous surface on Crista intercotylaris and Olecranon. Impressio brachialis is almost unobservable in C1–C12, and present with indistinct distal margin in C13. Foramina nutrientia is present on Margo interosseus at various positions on the proximal half, double in C7 and C8, single in all others, with large opening (5.3 × 1.0 mm in maximum). Papillae remigales caudales are absent (but observable on periosteum in live bird) in C1–C12, and eight prominent papillae observable (as ossified structures) in C13. Papillae remigales ventrales are absent in all cases. Linea intermuscularis is absent in C1–C12, and present but less distinct in C13. Extremitas distalis ulnae is cartilaginous in C1–C12, and ossified in C13.

*Juvenile* — Shaft curvature is as in adults. Extremitas proximalis ulnae is ossified, but with porous surface on Cotylae dorsalis et ventralis. Distal margin of Impressio brachialis is somewhat less distinct than in adults. Foramen nutriens is present on Margo interosseus at around the two-fifth of the shaft from the proximal end, and is always single, with larger opening than that in adults (about 3.5 × 0.5 mm). Papillae remigales caudales, 13 papillae are present, with three distalmost papillae indistinct. Papillae remigales ventrales, 10 prominent papillae are present, with three distalmost papillae in adults unobservable. Linea intermuscularis is as in adult. Extremitas distalis ulnae, numerous foramina are present on Sulcus intercondylaris, Labrum condyli dorsalis, and Depressio radialis.

*Adult* — Extremitas proximalis ulnae is ossified, with few foramen on and around. All muscular/ligamental attachments on the proximal end are distinct. Foramen nutriens is present on Margo interosseus at around the two-fifth of the shaft from the proximal end, and is always single, with a minute opening (about 1.5 × 0.2 mm). Papillae remigales caudales, 13 prominent papillae are present. Papillae remigales ventrales, 13 prominent papillae are present. Linea inter-

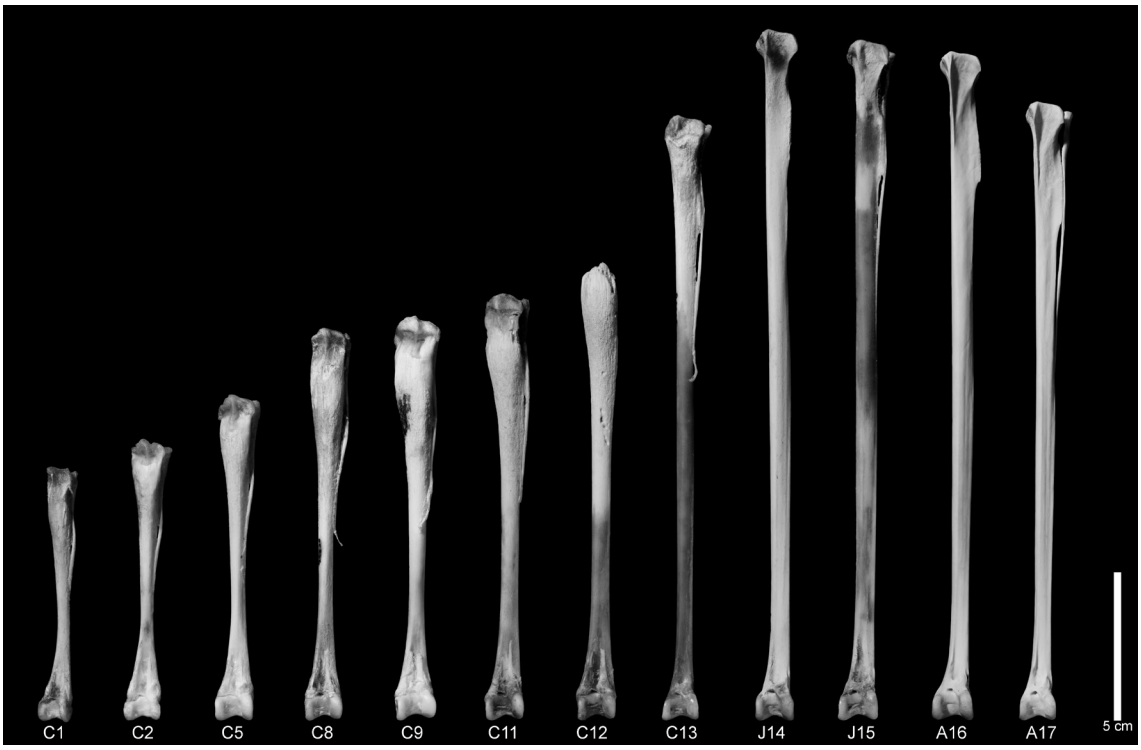


**FIGURE 5.** Ontogenetic morphological change of the tibiotarsus in *Ardea cinerea*. From left to right, C1, C2, C5, C8, C9, C11, C12 (proximal end damaged), C13, J14, J15, A16 and A17.

muscularis is present on the proximal region of Margo caudalis with a distinct ridge. Extremitas distalis ulnae, with occasional foramina on Sulcus intercondylaris, Labrum condyli dorsalis, and Depressio radialis.

**Carpometacarpus (Figs 4, 8A).** *Chick* — Five independent elements, including three metacarpi and two carpi, can be recognized; Os metacarpale alulare, Ossa metacarpale majus et minus, one carpus forming the proximal margin of Trochlea carpalis (dca in Fig. 8A), and another carpus for the distal margin of the ventral rim of Trochlea carpalis and the base of Processus pisiformis (dcb in Fig. 8A). The three metacarpi are ossified in all cases, and the two carpi are observable in C3 and larger. They are unfused to one another in C1–C12, but fused in C13. Margin of Trochlea carpalis is formed mostly by cartilage in C1–C10, formed mostly by unfused carpi in C11 and C12, and completely formed by fused carpi in C13. Processus pisiformis is not ossified in C1–C8, formed by one of the carpus (dcb in Fig. 8A) with cartilaginous tip in C9–C12, and ossified in C13. Sulcus tendineus is absent in C1–C12, and prominent throughout the distal one-third of the shaft in C13. Foramen nutriens is present on the caudal margin of Os metacarpale majus at around the midpoint, with moderate size of opening (about 1.0 × 0.5 mm). Almost no trace of muscular/ligamental attachments is observable in C1–C12: most of them are observable in C13, but less distinct than in juveniles and adults. Extremitas distalis carpometacarpi is cartilaginous in C1–C12, and ossified to form Symphysis metacarpalis distalis in C13.

*Juvenile* — All elements are completely ossified and fused (Fig. 8A). On Extremitas proximalis carpometacarpi, numerous foramina are present along the base of Os metacarpale alulare and around Processus pisiformis. Trochlea carpalis, Processus pisiformis, and Sulcus tendineus are ossified as in adults. Foramen nutriens is present on the caudal margin of Os metacarpale majus at around the midpoint, with moderate size of opening (about 0.6 × 0.3 mm). Extremitas distalis carpometacarpi is ossified, and foramina are present in Sulcus interosseus and on Facies articularis digitalis major.

*Adult* — All elements are completely ossified


**FIGURE 6.** Ontogenetic morphological change of the tarsometatarsus in *Ardea cinerea*. From left to right, C1, C2, C5, C8, C9, C11, C12, C13, J14, J15, A16 and A17.

and fused (Fig. 8A). On Extremitas proximalis carpometacarpi, a distinct foramen is present in Fossa infratrochlearis, and foramina can be present along the base of Os metacarpale alulare. Trochlea carpalis and Processus pisiformis are well marked. Sulcus tendineus is well marked throughout the distal half of the shaft. Foramen nutriens is present on the caudal margin of Os metacarpale majus at around the midpoint, with minute opening (about 0.2 × 0.2 mm). Extremitas distalis carpometacarpi is ossified, with few foramina in Sulcus interosseus. Foramina can be present on Facies articularis digitalis major.

**Femur** (Figs 4, 7C, 7D). *Chick* — Both ends can be either cartilaginous, with epiphysial ossification centers, or ossified. Extremitas proximalis femoris is cartilaginous with slight indication of Caput femoris on the ossified shaft in C1–C11 (femur of C12 was not available), and ossified but silghtly porous in C13. In C10 and C11, an irregularly-shaped ossification center is present in the proximal tip of cartilaginous Trochanter femoris (poc in Fig. 7C). Impressiones mm. et ligg. trochanteris are absent in C1–C10, only the distalmost one of them is observable in C11, and all are present but the proximalmost one is indistinct in C13. Linea intermuscularis cranialis is absent in C1–C11, and indistinct in C13. Lineae intermusculares caudales are absent C1–C11, and the medial one (on caudal margin) is blunt and the lateral one (on the caudolateral margin) is indistinct in C13. Foramina nutrientia are present on Facies caudalis et medialis, with various size of openings (2.0 × 1.0 mm in maximum). The tuberculum for Ansa m. iliofibularis is absent in C1–C10, indistinct in C11, and present as in adults in C13 (ta in Fig. 7D). Extremitas distalis femoris is entirely cartilaginous in C1–C3, containing an ossification center in C4–C11 (doc in Fig. 7D), and ossified with porous surface in C13 (Fig. 7D); the ossification center appears in cartilaginous Condylus medialis in C4, then expands to form Condyli lateralis et medialis and Trochlea fibularis in C10 and C11, and fuses with the diaphysis with little trace of suture in C13.

*Juvenile* — Both ends are ossified. On Extremitas proximalis femoris, numerous foramina sometimes present in Fovea lig. capitis and the craniolateral margin of Facies articularis antitrochanterica. Impressiones mm. et ligg. trochanteris are as in adults. Lineae intermusculares cranialis et caudales are as in adults. Foramina nutrientia are present on Facies caudalis et medialis, with various size of openings (2.0 × 0.5 mm in maximum). The tuberculum for Ansa m. iliofibularis (ta in Fig. 7D) is developed as in adults. Extremitas distalis femoris is almost completely

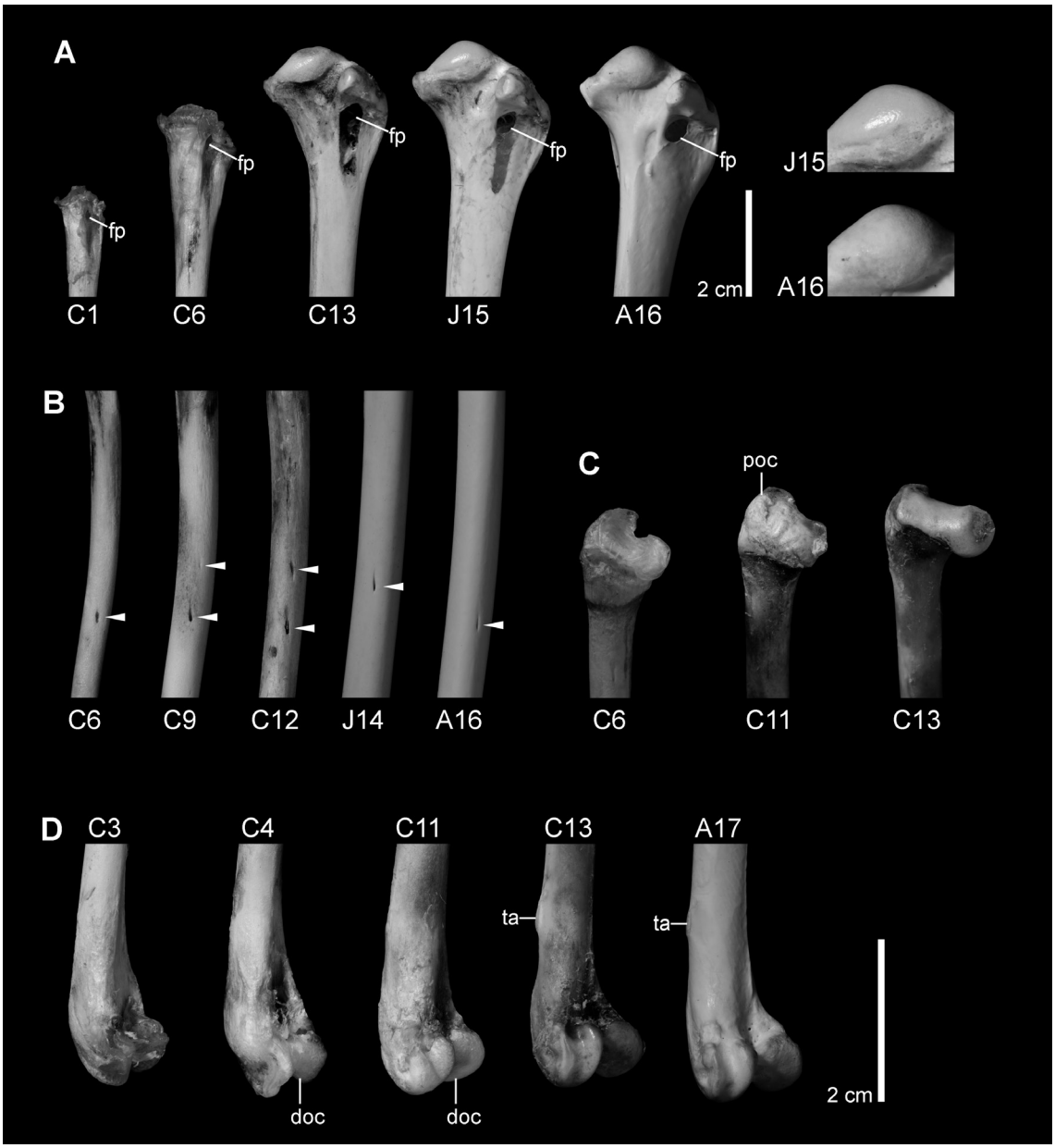


**FIGURE 7.** Ontogenetic morphological change in humerus and femur. **A**) proximal end of humerus, caudoventral view, in C1, C6, C13, J15 and A16 (from left to right). Caput humeri in J15 and A16 are magnified in the right insets. Foramen pneumaticum (fp) can be observed on the cartilaginous epiphysis in C1 and C6; in C13, periosteum is removed to show the opening of Foramen pneumaticum extending distally to form a fossa; and in J15, periosteum covering the fossa is left as it was in live bird. Note the porous nature of the margin of Caput humeri in J15 compared to that in A16 (right insets). **B**) ventral margin of humeral shaft, ventral view, in C6, C9, C12, J14 and A16 (from left to right). Positions of Foramina nutrientia are indicated by white arrowheads. Scale as in A. **C**) proximal end of femur, caudoproximal view, in C6, C11 and C13 (from left to right). In C6, proximal end is completely cartilaginous; in C11, an ossification center (poc) is present in cartilaginous Trochanter femoris; and in C13, proximal end is ossified. Scale as in D. **D**) distal end of femur, laterocaudal view, in C3, C4, C11, C13 and A17 (from left to right). In C3, distal end is completely cartilaginous; in C4 and C11, an ossification center (doc) is present to form distal condyles; and in C13 and A17, distal end is completely ossified. The tuberculum for Ansa m. iliofibularis (ta) is also shown.

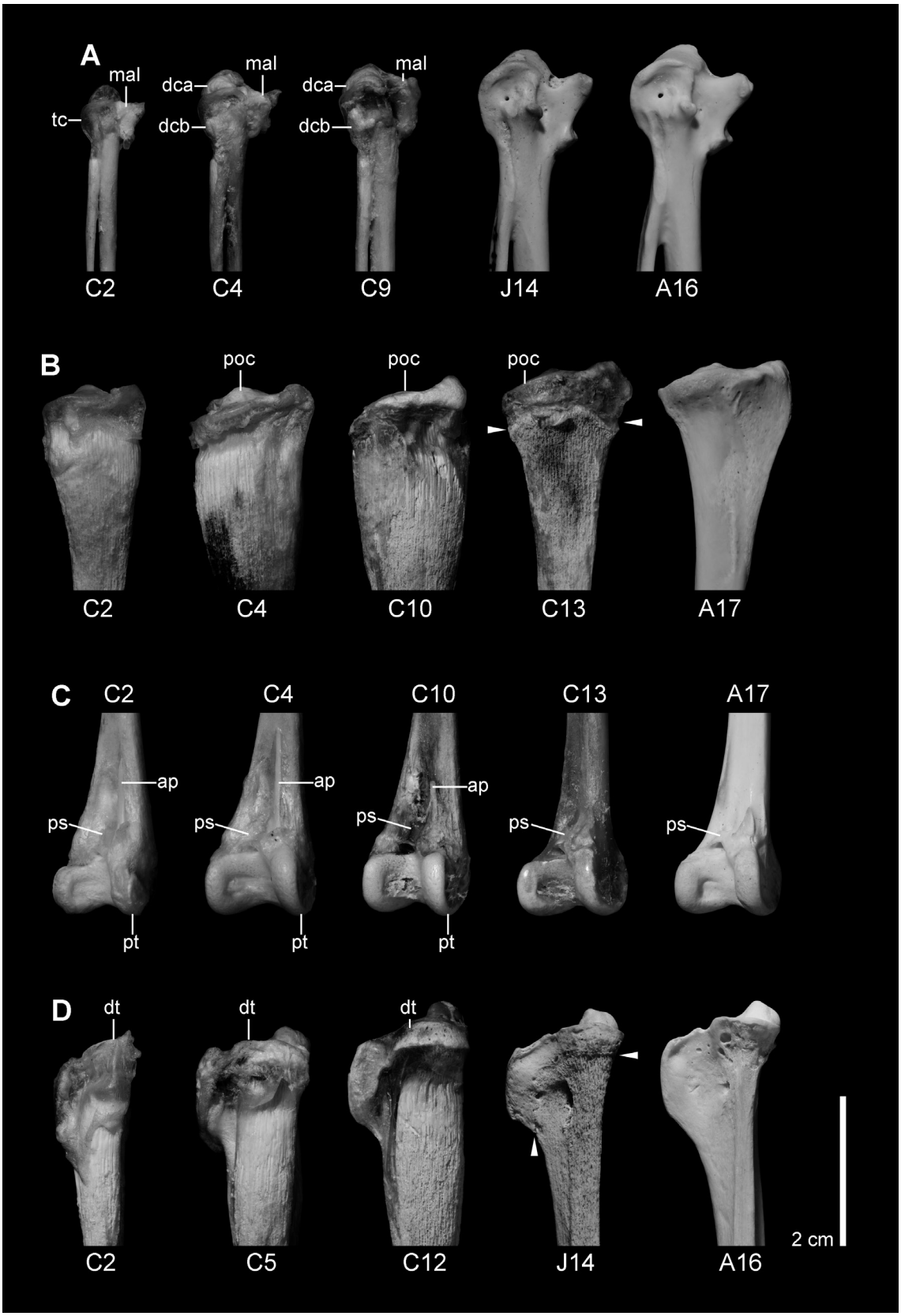
A
mal
tc
dca
dcb
C2
C4
C9
J14
A16
B
poc
C2
C4
C10
C13
A17
C
ap
ps
pt
D
dt
C5
C12
2 cm

ossified with no trace of suture; prominent foramina are occationally present in Sulcus patellaris and Fossa poplitea.

*Adult* — Both ends are ossified. On Extremitas proximalis femoris, several foramina are present on each of Fovea lig. capitis, cranial surface of Collum femoris, the area just medial to Trochanter femoris, and the caudal surface just distal to Facies articularis antitrochanterica. Impressiones mm. et ligg. trochanteris are distinct, with five scars observable. Linea intermuscularis cranialis is present, and running obliquely from Crista trochanteris toward Condylus medialis. Lineae intermusculares caudales are present on the caudal and caudolateral margins of the shaft. Foramina nutrientia are present on Facies caudalis et medialis, with minute openings (less than 1.0 × 0.4 mm). The tuberculum for Ansa m. iliofibularis is present on the distal region of the craniolateral margin of the shaft (ta in Fig. 7D). Extremitas distalis femoris is completely ossified with no trace of suture (Fig. 7D); minute foramina and a large foramen are present in Fossa poplitea.

**Tibiotarsus** (Figs 5, 8B, 8C). *Chick* — The shaft is generally wide and deep proximally. Extremitas proximalis tibialis is entirely cartilaginous in C1–C3, and cartilaginous with a distinct epiphysial ossification center in C4–C13 (poc in Fig. 8B); the ossification center appears in cartilaginous Area interarticularis of Caput tibiae, extends first laterally (from C6) then caudally (from C9) to form ossified Caput tibiae, and in C13 it is about to fuse with diaphysis with a distinct suture (Fig. 8B). The shaft distal to Caput tibiae is first flaring distally and then tapering distally to midshaft in C1–C12, and tapering relatively less steeply than in adults to the midshaft in C13. Crista cnemialis cranialis and Crista fibularis are indistinct and continuous with the shaft. Facies gastrocnemialis is convex. Fossa flexoria is absent. Foramen nutriens is present on the caudal side of Margo lateralis with an opening forming a large fossa (often more than 20.0 × 1.0 mm). On Extremitas distalis tibiotarsi, fused Ossa proximalia tarsi are observable as a single ossification center in the cartilaginous epiphysis in C1–C10 (pt in Fig. 8C), the tarsi are about to fuse to diaphysis of tibia with a distinct suture in C11 and C12, and the tarsi are fused to diaphysis of tibia with little trace of suture in C13. Condyli lateralis et medialis are cartilaginous caudally in C1–C3, and overall shape is formed by tarsi but surface porous with fine foramina in C4–C13 (Fig. 8C). Pons supratendineus (ps in Fig 8C) is a cartilaginous bridge between the "ascending process" (ap in Fig. 8C) of fused tarsi and diaphysis of tibia in C1–C12, and ossified in C13 (Fig. 8C).

*Juvenile* — The shaft is slender, relatively uniform in width and depth. Extremitas proximalis tibiotarsi is ossified with no trace of suture, with overall shape similar to adult; porous surface with numerous foramina dominates the area on and around Caput tibiae. Crista cnemialis cranialis is indistinct with the distal margin fading. The area between Crista cnemialis cranialis and Crista fibularis is almost flat. Foramen nutriens is present on the caudal side of Margo caudalis with an opening forming a slender fossa extending proximally (more than 7.0 × 0.7 mm). Extremi-

**FIGURE 8.** Ontogenetic morphological change in carpometacarpus, tibiotarsus and tarsometatarsus. **A**) proximal end of carpometacarpus, ventral view, in C2, C4, C9, J14 and A16 (from left to right). In C2, Os metacarpale alulare (mal) is the only ossified element in the proximal end, and Trochlea carpalis (tc) is cartilagenous; in C4 and C9, two carpi (dca and dcb) can be observed in proximal and distal portion of Trochlea carpalis, respectively. All elements are fused in J14 and A16. **B**) proximal end of tibiotarsus, medial view, in C2, C4, C10, C13 and A17 (from left to right). In C2, proximal end is completely cartilaginous; in C4 and C10, an ossification center (poc) is present to form (part of) the proximal articular surface; in C13, the ossification center is about to fuse with diaphysis of tibia with a distinct suture (white arrowheads); in A17, proximal end is completely ossified. **C**) distal end of tibiotarsus, craniolateral view, in C2, C4, C10, C13 and A17 (from left to right). In C2, C4 and C10, Ossa proximalia tarsi (pt) can be observed as a single ossification center, and form distal condyles, and Pons supratendineus (ps) is a cartilagenous bridge between diaphysis of tibia and the "ascending process" (ap) of Ossa proximalia tarsi; in C13 and A17, Ossa proximalia tarsi are fused to diaphysis of tibia. **D**) proximal end of tarsometatarsus, medial view, in C2, C5, C12, J14 and A16 (from left to right). In C2, C5 and C12, Os distale tarsi (dt) is present in the cartilaginous proximal end and Hypotarsus; In J14, it is fused to shaft of fused metatarsi with a distinct suture (white arrowheads); in A16, the suture is less obvious.

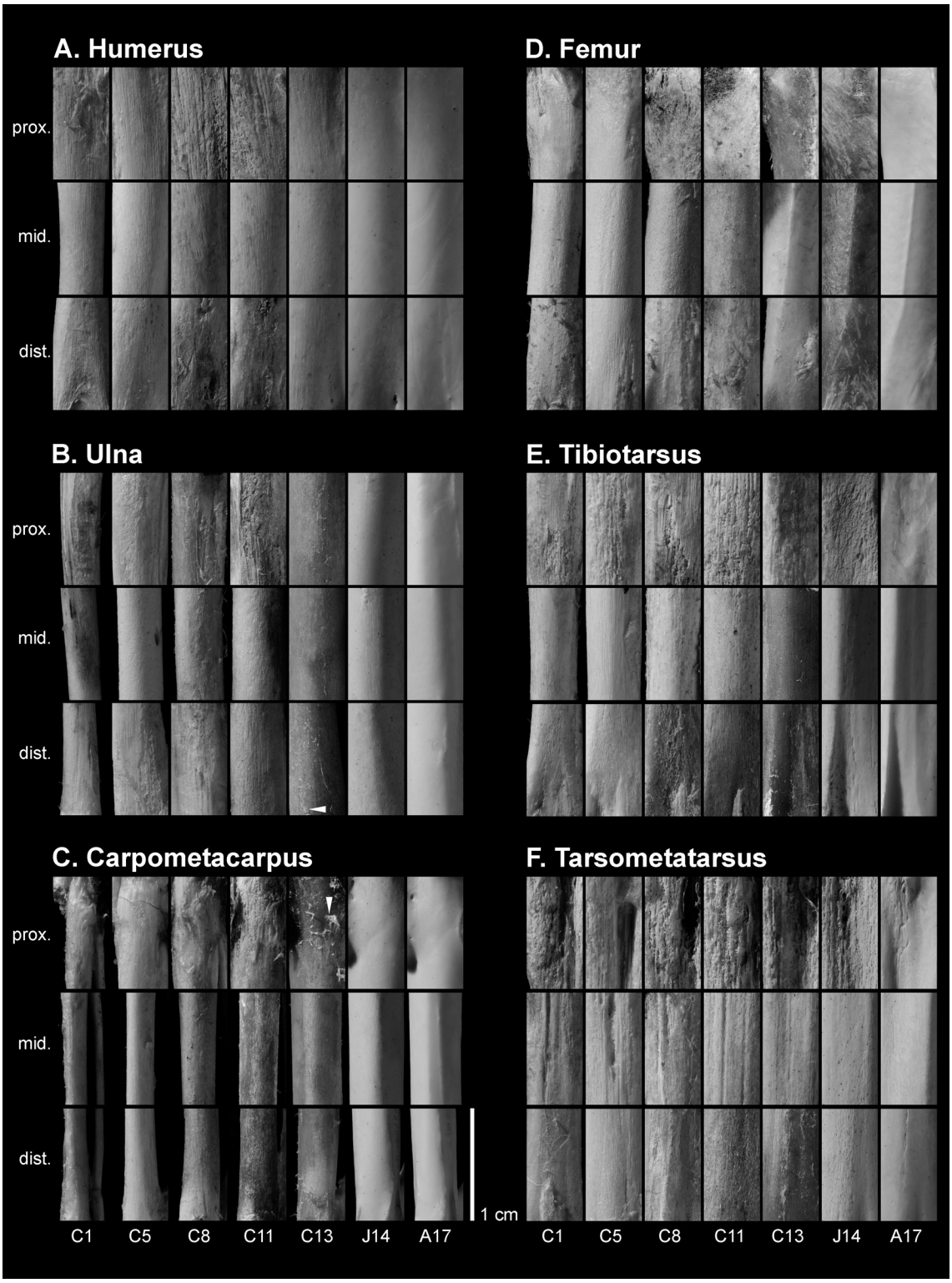


**FIGURE 9.** Bone surface textures on selected regions of long bones through ontogeny. **A**) humerus, **B**) ulna, **C**), carpometacarpus (Os metacarpale majus for the midshaft region), **D**) femur, **E**) tibiotarsus and **F**) tarsometatarsus. For each bone, proximal, midshaft and distal regions (from top to bottom) in C1, C5, C8, C11, C13, J14 and A17 (from left to right) are shown. Note the occasional presence of periosteum remains, which give fluffy appearance (see white arrowheads in the distal region of ulna and the proximal region of carpometacarpus in C13 for examples).

tas distalis tibiotarsi is ossified with no trace of suture; numerous foramina are present on medial surface of Condylus medialis and lateral surface of Condylus lateralis, and in Incisura intercondylaris and Sulcus extensorius.

*Adult* — The shaft is slender, with relatively uniform width and depth. On Extremitas proximalis tibiotarsi, numerous minute foramina are present on and around the margin of Caput tibiae (Fig. 8C). Facies gastrocnemialis and Fossa flexoria are sloping steeply from Caput tibiae to the shaft. Crista cnemialis cranialis is well developed with distal margin reaching distally to the position of the midpoint of Crista fibularis. The area between Crista cnemialis cranialis and Crista fibularis is flat to somewhat concave. Foramen nutriens is present on the caudal side of Margo caudalis with a long but thin opening (about 5.0 × 0.2 mm). Extremitas distalis tibiotarsi is ossified with no trace of suture (Fig. 8C); numerous minute foramina are present on medial surface of Condylus medialis and lateral surface of Condylus lateralis, and in Incisura intercondylaris.

**Tarsometatarsus** (Figs 6, 8D). *Chick* — The shaft is extremely broad proximally, with width and depth reducing gradually distally, and the depth is relatively uniform mediolaterally. Extremitas proximalis tarsometatarsi and Hypotarsus are cartilaginous, with ossified Os distale tarsi within them in C1–C12 (dt in Fig. 8D). Os distale tarsi is observable as a single ossification center, forming first Extremitas proximalis tarsometatarsi (from C1) and then Hypotarsus (from C4), and fusing to the shaft of the fused metatarsi in C13. Sulcus extensorius is broad with blunt margins. Foramina vascularia proximalia are very long, reaching to the proximal epiphysial cartilage in C1–C12. Tuberositas m. tibialis cranialis is almost unobservable. The rims of Trochleae metatarsorum II, III et IVare cartilaginous in C1–C8, mostly ossified but porous in C9–C12, and almost completely ossified in C13.

*Juvenile* — The shaft is relatively slender, width reducing gradually distally from the proximal suture then maintaining uniform width, and depth shallowing medially and slightly distally. Extremitas proximalis tarsometatarsi and Hypotarsus are ossified, and Os distale tarsi is fused with the fused metatarsi with a distinct suture (Fig. 8D). The area between Extremitas proximalis tarsometatarsi and the suture line is uniform in width unlike in adults where the area is tapering distally, and with numerous foramina. Margins of Sulcus extensorius are less developed cranially than in adults and fading proximal to the midpoint of the shaft. Foramina vascularia proximalia are long (the dorsal openings are more than 4 mm in longitudinal length). Tuberositas m. tibialis cranialis is indistinct. Trochleae metatarsorum II, III et IV are as in adults.

*Adult* — The shaft is slender, its width is tapering from the position just distal to the margin of Extremitas proximalis tarsometatarsi and then relatively uniform throughout the shaft, and its depth is deepest proximolaterally, shallower medially and tapering gradually distally. Extremitas proximalis tarsometatarsi and Hypotarsus are ossified with no trace of suture, with large surrounding foramina (Fig. 8D). Margins of Sulcus extensorius are well developed and extending distal to the midpoint of the shaft. Foramina vascularia proximalia are short longitudinally (the dorsal openings are about 1.5 mm in longitudinal length). Tuberositas m. tibialis cranialis is prominent. Trochleae metatarsorum II, III et IV are completely ossified with few foramina on and around.

## Surface texture

Surface textures of long bones showed considerable variation among developmental stages. They can also vary among elements within a single individual, and even within a single element. Surface textures of various regions of long bones are illustrated in Fig. 9, and longitudinal distribution of textural patterns of long bones, measured as described in Materials and Methods, in selected individuals are shown in Fig. 10. Results for individuals not shown did not differ considerably from those shown in the same developmental stage.

In general, long bones of chicks show rough surface textures (mostly patterns A–C), those of juveniles are smoother but weakly grooved and/or dimpled (mostly pattern D), and those of adults are smooth with little grooves or dimples (mostly

pattern E). Surface textures in smallest chicks (C1 and C2) can show a slightly smoother appearance than in larger ones; a striated structure with transverse struts (pattern B) was not observed in some bones, and fibrous/porous texture (pattern C) in the midshaft have less penetrating pits than in larger ones. Elements within a single individual show similar sorts of surface textures, but certain elements tend to have smoother or rougher surface textures than other elements (see below). Within a single element, surface texture is relatively uniform transversely, and is much more variable longitudinally. Generally, loose, striated texture and rough surface (patterns A and B) appear near proximal and distal epiphyses (especially when the epiphysis is not ossified), then they are replaced by less rough fibrous texture diaphysially (typically patterns C and D), and the density of grooves and dimples are least in midshaft region (Fig. 9). Specific characteristics of each element are described below.

*Humerus* (Figs 9A, 10A) — Humeri show the typical ontogenetic variation described above. In most chicks, C1–C12, surface texture can be classified into either patterns A, B or C, whereas in the largest chick observed, C13, surface texture shows few penetrating pits through most of the shaft, thus classified as pattern D. Longitudinal grooves, rather than dimples, are common in the midshaft region. The proximal shaft, especially caudal surface of Crista deltopectoralis, shows rougher surface texture compared to other part. Numerous distinct penetrating pits can be observed in the area proximal to Fossa m. brachialis (Fig. 9A; bottom row). In juveniles, surface texture is overall smooth, but with faint grooves (pattern D). In adults, surface texture is smooth with few grooves or dimples (pattern E).

*Ulna* (Figs 9B, 10B) — Overall pattern of ontogenetic variation of surface texture in ulnae is similar to that described in the humerus. The area occupied by striated structure (patterns A and B) is relatively long in the distal end. In both ends, the area of pattern A extends further toward diaphysis in convex caudal margin, whereas it is immediately replaced by pattern B in concave cranial margin. In C13 and J14, the areas next to both ends show slightly fibrous texture with penetrating pits (pattern C). In J15, the shaft is almost entirely without penetrating pits (pattern D), and in adults it is overall smooth (pattern E).

*Carpometacarpus* (Figs 9C, 10C) — Carpometacarpi show little deviation from the typical ontogenetic variation described above. Both Ossa metacarpi majus et minus show similar sort of patterns. In the midshaft region in chicks, dimples are more common than longitudinal grooves.

*Femur* (Figs 9D, 10D) — Femora show somewhat smoother surface textures when compared to other bones of the same individual. In chicks, patterns A and B are restricted to small areas near epiphyses. In C10 and C11, surface texture with few penetrating pits (pattern D) can be observed, contrasting to other elements in the individuals. In the midshaft region, few longitudinal grooves appear and dimples dominate. In C13, J14 and J15, all of the shaft is occupied by a texture with numerous faint dimples and little penetrating pits (pattern D). In adults, the shaft is entirely smooth (pattern E).

*Tibiotarsus* (Figs 9E, 10E) — Tibiotarsi show pronounced intra-elemental variation of surface textures. In chicks, striated structures (patterns A and B) occupy most of the surface on the flared proximal shaft, giving larger proportions within the bone than most other bones. Rough surface textures (patterns B and C) persist in the proximal region until juvenile stage (J14 and J15), unlike most other bones. The distal shaft is relatively smoother, and there is a distinct area with few penetrating pits (pattern D) in the region in C12. In rough surfaces of the proximal to midshaft regions, longitudinal grooves are more common than dimples, whereas in the distal region dimples are more common. The entire shaft is occupied by smooth surface texture (pattern E) in adults.

*Tarsometatarsus* (Figs 9F, 10F) — Tarsometatarsi show considerable intra-elemental variation, even in juvenile and adult stages. In chicks, the flared proximal shaft is occupied by striated structures (patterns A and B), as in the tibiotarsus. The striated structure with transverse struts (pattern B) also appears in the proximal shaft in juveniles. Even in C13, J14 and J15, where the shaft of most other elements have surface texture with few penetrating pits (pattern D), the pattern appears only in the distalmost shaft. In adults, smooth surface texture (pattern E) appears only in the distalmost shaft, and large proportion

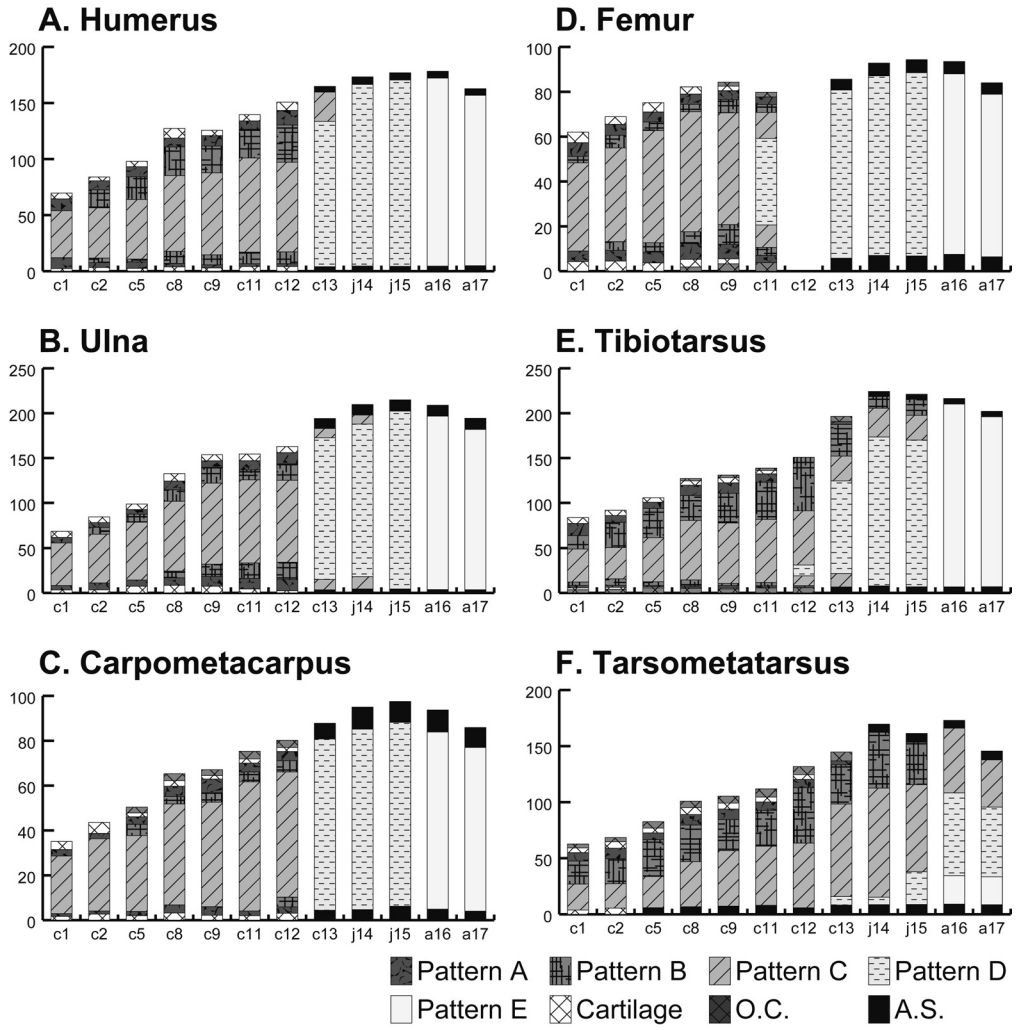


**FIGURE 10.** Longitudinal distributions of surface textural patterns in six long bones through ontogeny. A) humerus, B) ulna, C), carpometacarpus (Os metacarpale majus), D) femur, E) tibiotarsus and F) tarsometatarsus. For each bone in selected individuals (same ones as in Figs 2–6), longitudinal distributions of patterns A to E, as well as epiphysial cartilages, ossification centers (O.C.) and articular surfaces (A.S.), are shown with distal end at bottom. Vertical axes in millimeter (mm). See Materials and Methods for the definition and measurement of longitudinal distribution of patterns.

is occupied by textures with faint longitudinal grooves (patterns C and D). Longitudinal grooves are common in rough surface in chicks and juveniles. In adults, they are relatively rare and short in length.

## Discussion

**Ontogeny of long bones.** In the study series of the Gray Heron (*Ardea cinerea*), macroscopic morphology and surface textures of all six long bones show ontogenetic variation. Long bones show various degrees of change in linear dimensions (Figs 2–6, Tab. 2). In general, they increase gradually through the chick stage and reach adult size range as early as the time of fledging (except for tibiotarsus and tarsometatarsus, where length of each bone of the largest chick are slightly smaller than that in older individuals), although some dimensions of shaft thickness of leg bones reach their peak before this time and then decrease (see below for further discussion). Epiphysial areas of long bones are cartilaginous and can contain a distinct ossification center through most of the

chick stage. Most of epiphyses are ossified at or slightly before the time of fledging (C13; with the exceptions of the proximal ends of tibiotarsi and tarsometatarsi, where complete fusions occur between C13 and J14), but they show slightly more porous surface than adults until the juvenile stage. Epiphysial areas are completely ossified in adult stage (Figs 2–8). Most osteological landmarks and muscular/ligamental attachment scars are not observable as ossified structures through most of the chick stage. At fledging they are more or less observable on the ossified area, but margins are less distinct than in the later stages. In the juvenile stage, they are mostly similar to those in the adult stage, although there are distinct ontogenetic changes between the two stages in some features including Foramen pneumatica of humerus and Crista cnemialis cranialis of tibiotarsus (Figs 2–8). Distinctly large Foramina nutrientia on bone walls in chicks

**TABLE 3.** Summary of proportions of longitudinal distributions of five textural patterns in six long bones through ontogeny. Proportions of longitudinal distributions of patterns A to E are expressed in percent (%) to the ossified length of the bone. For each combination of long bones and developmental stages, minimum and maximum values among individuals (C, chick; J, juvenile; A, adult) are shown. $N = 13$ for chicks (12 for femur), 2 for juveniles and 2 for adults. See Materials and Methods for the definition and measurement of longitudinal distribution of patterns.

| | A | B | C | D | E |
|---|---|---|---|---|---|
| **Humerus** | | | | | |
| C | 0.0–32.5 | 0.0–31.6 | 16.8–67.5 | 0.0–83.2 | 0.0 |
| J | 0.0 | 0.0 | 0.0 | 100.0 | 0.0 |
| A | 0.0 | 0.0 | 0.0 | 0.0 | 100.0 |
| **Ulna** | | | | | |
| C | 0.0–19.1 | 0.0–29.9 | 12.2–81.1 | 0.0–87.8 | 0.0 |
| J | 0.0 | 0.0 | 0.0–12.3 | 87.7–100.0 | 0.0 |
| A | 0.0 | 0.0 | 0.0 | 0.0 | 100.0 |
| **Carpometacarpus** | | | | | |
| C | 0.0–17.6 | 0.0–13.0 | 0.0–89.4 | 0.0–100.0 | 0.0 |
| J | 0.0 | 0.0 | 0.0 | 100.0 | 0.0 |
| A | 0.0 | 0.0 | 0.0 | 0.0 | 100.0 |
| **Femur** | | | | | |
| C | 0.0–20.4 | 0.0–19.6 | 0.0–75.7 | 0.0–100.0 | 0.0 |
| J | 0.0 | 0.0 | 0.0 | 100.0 | 0.0 |
| A | 0.0 | 0.0 | 0.0 | 0.0 | 100.0 |
| **Tibiotarsus** | | | | | |
| C | 1.6–22.1 | 19.1–43.9 | 23.2–57.9 | 0.0–55.8 | 0.0 |
| J | 0.0 | 6.2–8.6 | 13.2–15.2 | 78.2–78.6 | 0.0 |
| A | 0.0 | 0.0 | 0.0 | 0.0 | 100.0 |
| **Tarsometatarsus** | | | | | |
| C | 2.6–17.4 | 27.3–54.5 | 33.9–64.1 | 0.0–6.0 | 0.0 |
| J | 0.0 | 26.1–32.4 | 53.7–63.2 | 4.4–20.2 | 0.0 |
| A | 0.0 | 0.0 | 32.6–36.8 | 47.1–48.1 | 16.1–19.3 |

(Fig. 7B) could be correlated to active blood flow and bone metabolism (see Seymour *et al.* (2012) and references therein). The occasional presence of Foramen nutriens covered by thin bone wall indicate that they can be opened or closed during ontogeny. Surface textures of long bones also show considerable ontogenetic change. Through most of the chick stage, fibrous/porous surface texture with frequent penetrating pits (pattern C) dominates in the midshaft region, whereas striated structures (patterns A and B) dominate near both epiphyses of long bones (with some exceptions). In larger chicks, smoother surface texture with faint grooves/dimples and few penetrating pits (pattern D) appears in the midshaft region of femur and the distal shaft of tibiotarsus. At the time of fledging, rough surface textures (patterns A and B) are mostly replaced by smoother one (pattern D) with occasional remains of rougher textures on epiphysial areas (particularly in the proximal regions of tibiotarsus and tarsometatarsus). This state persists through the juvenile stage. In the adult stage, smooth surface texture with few grooves/dimples (pattern E) dominates on all long bones except for tarsometatarsus, where rougher surface (patterns C and D) occupies considerable portion of overall area (Figs 9 and 10). Proportions of longitudinal distribution of surface texture patterns, expressed as a percentage to ossified length of a bone, in each developmental stage are summarized in Tab. 3.

The presence of inter-elemental variation of surface textures among six long bones results in differences in relative timing of the appearance of smooth surface textures. Of the six elements examined, the femur is the first element to attain pattern D (in C10), the tibiotarsus is the second (in C12; although limited to the distal shaft), and all others follow (in C13). Rough surface textures (patterns A–C) disappear earliest in the carpometacarpus and femur (at latest in C13), followed by the humerus (in J14), ulna (in J15), and tibiotarsus (in A16), and persist through all of the series in tarsometatarsus. One possible reason for the tarsometatarsus to retain relatively rough surface texture (patterns C and D) in the adult stage is that it is firmly attached to podotheca (Baumel & Witmer 1993). It is notable that the proximal ends of tibiotarsus and tarsometatarsus, where complete ossification of epiphysis occurs later than in the other bones, retain rougher surface until later period of development. This fact, along with longitudinal distribution of surface textures in long bones, suggests that striated structures (patterns A and B) might be partly relevant to active longitudinal growth of long bones, as well as bone remodeling process. The possible biological significance of this inter-elemental variation is further discussed below.

The combination of observations on surface textures and histology of long bones in the Canada Goose (*Branta canadensis*) have revealed that rough surface textures on long bones are underlain by actively growing fibrolamellar bone tissue, characterizing immature long bones (Tumarkin-Deratzian *et al.* 2006). Their discussion is based primarily on estimated relative developmental stages of the samples, which are based mainly on possession of osteological landmarks, with several other supportive evidences (length of the bones, and date of death of individuals). The current study, based on originally prepared specimens of the Gray Heron (*Ardea cinerea*), confirms that lack of osteological landmarks and rough surface textures do occur in the immature chick stage. It is remarkable that most individual surface textures observed in *Ardea* in the current study (Figs 1 and 9), such as a rough striated texture with frequent transverse struts (pattern B), a fibrous/porous texture with frequent longitudinal grooves/dimples (pattern C), and a smooth texture with few longitudinal grooves/dimples (pattern E), are almost qualitatively identical to those observed in *Branta* in Tumarkin-Deratzian *et al.* (2006: figs 5–7).

In addition, the overall pattern of transition of surface texture from striated, fibrous texture into smooth surface observed in *Ardea cinerea* is similar to that reported by Tumarkin-Deratzian *et al.* (2006) in *Branta canadensis*. They defined seven texture types, type I to VII in the order of decreasing degree of roughness, to describe the overall composition of surface textures of a long bone, which are considered to represent relative developmental stages within each element. According to their definition of texture types (Tumarkin-Deratzian *et al.* 2006: pp. 143–148 and tab. 6), long bones of the study series of *Ardea cinerea* in the current study can be classified as in Tab. 4. Although some of the seven

texture types could not be recognized in the study series of *Ardea cinerea*, the table shows that the ontogenetic sequence of surface texture types observed in *Ardea* is consistent with that identified in *Branta*, confirming the previous authors' hypothesis that "ontogenetic patterns of bone texture change in other species may be similar to those observed in *B. canadensis*" (p. 159). This similarity confirms the reliability of surface textures as a ageing criterion for bird fossils.

According to Tumarkin-Deratzian *et al.* (2006), bones of birds that have not yet reached the adult size range show texture type I; birds that have reached adult size ranges but are not yet fully skeletally mature show texture types II–V; and birds attained both adult size and skeletal maturity show texture types VI and VII. This statement appears roughly true also in *Ardea cinerea*, where all bones of chicks that have not yet reached the adult size range (C1–C12) show texture type I, and most bones of birds that attained adult size range (C13–J15) show texture types III and IV. However, it should be noted that rough striated surface textures, whose presence define texture type I, can be observed in the proximal shaft of tibiotarsi and tarsometatarsi of those that have reached adult size range (C13–J15). This fact does not significantly diminish the reliability of surface textures as a criterion for ontogenetic ageing because the overall pattern of transition is quite consistent for each bone. But the presence of such inter- and intra-elemental variation should be taken in mind when dealing with isolated/fragmental fossil bones. Tumarkin-Deratzian *et al.* (2006) also concluded, from the distribution of textural maturity against date of death, that adult surface with grossly smooth texture (texture types VI and VII) is attained in the winter of the hatching year in that species. Unfortunately, as the two juveniles available to this study were both collected in the first summer (June and August; Tab. 1), exact timing of attaining smooth surface in *Ardea* could not be determined in this study.

**Inter-elemental variation.** One interesting difference between ontogenies of surface textures of long bones in *Ardea cinerea* (this study) and *Branta canadensis* (Tumarkin-Deratzian *et al.* 2006) is found in inter-elemental difference of relative timing of attaining mature surface textures. Tumarkin-Deratzian *et al.* (2006) examined sur-

**TABLE 4.** Texture types (Tumarkin-Deratzian *et al.* 2006) applied to the long bones of *Ardea cinerea*. Each long bone is classified into one of the seven texture types (types I to VII) according to the definition and description given by Tumarkin-Deratzian *et al.* (2006).

| | Humerus | Ulna | Carpometacarpus | Femur | Tibiotarsus | Tarsometatarsus |
|---|---|---|---|---|---|---|
| C1 | I | I | I | I | I | I |
| C2 | I | I | I | I | I | I |
| C3 | I | I | I | I | I | I |
| C4 | I | I | I | I | I | I |
| C5 | I | I | I | I | I | I |
| C6 | I | I | I | I | I | I |
| C7 | I | I | I | I | I | I |
| C8 | I | I | I | I | I | I |
| C9 | I | I | I | I | I | I |
| C10 | I | I | I | I | I | I |
| C11 | I | I | I | I | I | I |
| C12 | I | I | I | — | I | I |
| C13 | III | III | IV | IV | I | I |
| J14 | IV | III | IV | IV | I | I |
| J15 | IV | IV | IV | IV | I | I |
| A16 | VII | VII | VII | VII | VII | V |
| A17 | VII | VII | VII | VII | VII | V |

face textures of three long bones, humerus, femur and tibiotarsus, in *B. canadensis*, and pointed out the tendency of the humerus to retain immature rough surface textures longer than the other two bones in that species. In contrast, in *A. cinerea*, the tibiotarsus retains immature rough surface longer than humerus and femur (Figs 9 and 10, Tab. 4).

Assuming that attaining smooth surface texture corresponds to cessation of active bone growth, relative timing of attaining smooth surface texture can be regarded as relative timing of maturity among long bones. So it is likely that the relative timing of attaining smooth surface textures among long bones reflects some biological aspects of avian ontogeny, such as resource allocation among limb sections and allometric/heterochronic change in limb growth. There are two possible explanations for interspecific difference of the relative timing of attaining smooth surface textures between *Ardea cinerea* and *Branta canadensis*. First, the difference may reflect different locomotor requirements in early ontogeny between the two species. In the Family Anatidae, including *Branta*, chicks generally hatch in precocial condition, and have to walk and swim to follow the parents and to feed for themselves immediately after hatching (Starck & Ricklefs 1998; Bowler 2005). In order to achieve sufficient locomotor ability early in ontogeny, anatid chicks mature their hindlimbs much earlier than forelimbs and pectoral girdle (Hohtola & Visser 1998; Dial & Carrier 2012). In contrast, in the Family Ardeidae, including *Ardea*, chicks hatch in (semi-)altricial condition, in which they stay in the nest for a certain period (about six weeks in *Ardea cinerea*, when chicks can clamber away from nests to the forest canopy of the colony; Yamashina 1941) and are fed by their parents until fledging (at about seven to eight weeks old in *Ardea cinerea*, and 2–3 to 12–13 weeks among Ardeidae (Yamashina 1941, Starck & Ricklefs 1998; Kushlan & Hancock 2005). In this condition, hindlimbs would be released from drastic development in early ontogeny, allowing bone growth to continue until late ontogeny. Second, the difference could be related to the different proportion of limb sections between the two species, such as the extremely long distal leg in *Ardea*. If there exist any constraints on longitudinal growth rates in long bones (see Carrier & Auriemma 1992), extremely long leg bones in *Ardea* would need a longer time period to reach adult size. Of course, these two explanations are not mutually exclusive, and it is fairly possible that the difference results from both factors. Comparative studies with more sample taxa, including long-legged precocial species (*e.g.*, gruids, ratites, etc.), would be fruitful.

**Ossification centers.** The presence of epiphysial ossification centers in long bones of birds has not been widely accepted (see Baumel & Witmer 1993: Annotation 2; but see also Starck 1994: footnote in p. 121). In spite of repeated mentions to "epiphysis" by earlier authors (Latimer 1927; Huggins *et al.* 1942), Haines (1942) and Bellaris & Jenkin (1960) considered them as misidentifications. One exception is an ossification center in the proximal end of tibiotarsus. Hogg (1980) reported and figured a distinct ossification center at the cranial margin of the proximal end of tibiotarsus in the domestic fowl under the name of "proximal tibial centre" (pp. 735, 741, figs 11, 12, 14, 15) (but curiously his later study (Hogg 1982) did not mention it). Hall (2005) recognized its presence in the domestic fowl as a secondary ossification center, and considered it to be relevant to the rapid growth rate of tibiotarsus. Through a radiological study on a kiwi (*Apteryx australis mantelli*), Beale (1985, 1991) showed the presence of an ossification center at the equivalent position, and called it "patella" (Beale 1985: p. 190–191, fig. 5). Turvey & Holdaway (2005), studying ontogeny of the extinct Giant Moa (*Dinornis*), also figured and described this structure as "patella" (p. 73, fig. 3). A distinct ossification center in *Grus grus* from an archaeological site was figured by Serjeantson (1998). Recently, through their examination of osteological characters, Livezey & Zusi (2006) concluded that the ossification center at that position is not a patella but a distinct "tibial epiphysis" (p. 322).

The study series of *Ardea cinerea* clearly demonstrated the presence of a distinct epiphysial ossification center in the proximal tibiotarsus and supports Livezey & Zusi's (2006) view, because the ossification center in this species first appears

at the middle part of the articular surface, rather than at the cranial margin where the patellar tendon inserts (Fig. 8B). This ossification center then extends craniolaterad, and later caudad to form the entire Extremitas proximalis tibiotarsi. It apparently starts fusing with the diaphysis of tibia around fledging, and the suture disappears in the early juvenile stage. The study series also showed the presence of distinct epiphysial ossification centers in the proximal and distal ends of femur. To date, there appears to be no definite descriptions of them in the literature. The one in the proximal end of femur appears in the middle chick stage (C10) in the proximal margin of cartilaginous Trochanter femoris (Fig. 7C). The one in the distal end of femur appears earlier (in C4) at the caudal margin of the distal condyles, and then extends to form entire Extremitas distalis femoris (Fig. 7D). Unfortunately, the process of fusion of these ossification centers could not be observed. Both proximal and distal ends of femur are ossified at the time of fledging with little trace of sutures. It is not clear whether these ossification centers are induced in response to mechanical loadings (Carter *et al.* 1998) or not. Further studies are required to clarify phylogenetic distribution and histological nature of epiphysial ossification centers in birds.

**Bone growth.** Long bones grow both longitudinally and circumferentially. Longitudinal growth occurs through endochondral ossification in epiphyses, or in epiphysial growth plates (Wolbach & Hegsted 1952; Starck 1996), whereas circumferential growth occurs through membranous ossification, or direct deposition of new bone tissue on existing bone surface in periosteum (Bellaris & Jenkin 1960). In the ontogenetic series of *Ardea cinerea* observed in this study, most long bones of the largest chick studied, C13, have equivalent length to those in small adults studied (Figs 2–6, Tab. 2), suggesting that long bones reach adult size range in length during chick stage (except for tibiotarsus and tarsometatarsus). At the same time, both ends of long bones are ossified to retain no trace of epiphysial growth plates (except for the proximal ends of tibiotarsus and tarsometatarsus, where fusion of epiphysial ossification center and Os distale tarsi, respectively, with each diaphysis is completed slightly later). These two facts suggest that longitudinal growth of long bones in this species ceases at (or slightly after) the end of the chick stage, or the time birds become capable of flight and leave birth colonies.

In contrast, circumferential growth of long bones does not appear to cease at this time in *Ardea cinerea*. Almost all dimensions of shaft diameters in long bones are larger in all adults and juveniles than in largest chicks (except for shaft depth at the midpoint in femur; Tab. 2). Although the sample size is too small for statistical tests, it would be reasonable to suppose that circumferential growth of long bones continues for a certain period after cessation of longitudinal growth in this species. Rough surface textures in chicks and juveniles, indicating active bone growth (Tumarkin-Deratzian *et al.* 2006), support this hypothesis. Also, in the House Sparrow (*Passer domesticus*), it has been reported that most long bones of adults are significantly thicker, but not longer, than those of first year birds in females (though not in males; Bjordal 1987).

Interestingly, the proximal shafts of tibiotarsus and tarsometatarsus are considerably thicker in chicks than in juveniles and adults (Figs 5, 6, 8B, 8D, Tab. 2). These regions are characterized by extremely rough surface textures (Figs 9 and 10), suggesting active bone remodeling in these regions (see above). This fact strongly suggests that intensive resorption of bone tissue is taking place in the cortex of these leg bones in the ontogeny of *Ardea cinerea*. Although the exact significance of this resorption is not clear, one possible explanation is that the thick bone shaft in leg bones of *Ardea* chicks compensates for less dense, weak immature bone tissue, providing the leg bones with sufficient strength to sustain growing body weight. Carrier & Leon (1990) observed thick bone walls in leg bones of the California Gull (*Larus californicus*) chicks, and concluded thick bone walls might compensate for weak bone tissue in rapidly growing animals. Similar compensation might take place in the leg bones of *Ardea* chicks.

**Ontogenetic ageing in bird fossils.** Recent birds, in general, are considered to undergo rapid growth in early ontogeny and attain skeletal maturity within a year (*e.g.*, Padian *et al.* 2001).

As far as for surface textures of long bones, available data on skeletal ontogeny in *Branta canadensis* (Tumarkin-Deratzian *et al.* 2006) and *Ardea cinerea* (this study) are consistent with the idea. However, there are some exceptions. In kiwi (*Apteryx*), epiphyses of leg bones may retain unfused independent ossification centers for more than four years (Beale 1985, 1991), and histological studies revealed that they undergo cyclical interrupted growth for five to six years (Bourdon *et al.* 2009). Similar growth pattern have been suggested for extinct moas (Turvey *et al.* 2005; Turvey & Holdaway 2005). It should also be noted that some basal birds are likely to have had distinct growth strategies than modern birds, in which cortical bone deposition is frequently interrupted (Chinsamy-Turan 2005).

Through the study of both surface textures and histology of long bones in the American Alligator (*Alligator mississippiensis*), Tumarkin-Deratzian *et al.* (2007) showed that an apparently smooth surface texture can occur on the long bones of immature individuals in animals with cyclical interrupted growth, and cautioned that textural ageing on fossil animals with unknown growth strategies would be problematic. At this time, textural ageing on fossil birds with unknown or interrupted growth strategies should be similarly problematic, as there are no detailed data on ontogenetic change of surface texture in birds with interrupted growth or longer growth periods. Clearly more studies are needed to establish reliable ageing criteria for bird fossils.

## Conclusion

Postnatal ontogenetic changes of macroscopic morphology and surface texture in major long bones of the Gray Heron (*Ardea cinerea*) were described and illustrated. Both macroscopic morphology and surface texture of each element showed relatively consistent shifts through ontogeny, and thus these changes would be useful in ontogenetic ageing of fossil bird materials. Long bones of chicks are typically characterized by indistinct muscular/ligamental attachments and cartilaginous epiphyses. Those of adults are characterized by distinct muscular/ligamental attachments and completely ossified epiphyses. Those of juveniles (here, birds under one-year-old) can be distinguished from adults by some qualitative characters, including articular surfaces with more porous margins, large nutrient foramina, Foramen pneumatica of humerus extending distally to form a fossa, less distinct distal Papillae remigales of ulna, less developed Crista cnemialis cranialis of tibiotarsus, and much larger Foramina vascularia proximalia of tarsometatarsus. Long bones of chicks typically have a striated surface texture near both epiphyses and rough fibuous/porous surface textures with distinct longitudinal grooves and/or dimples and penetrating pits in the midshaft. Those of juveniles are dominated by an overall smooth surface texture with faint longitudinal grooves and/or dimples and few penetrating pits; surface textures with frequent penetrating pits can remain near either or both epiphyses. Adult long bones are characterized by an overall smooth surface texture with few longitudinal grooves and dimples, except for tarsometatarsus.

However, there can be considerable variation of surface textures among elements even within a single individual. For instance, a rough striated structure can be observed on the proximal regions of tibiotarsus and tarsometatarsus in juveniles of *Ardea cinerea*, whereas their distal regions and most other elements show only faint grooves or dimples. The presence of such variation suggests that assessment of ontogenetic age of an individual based on a single isolated fossil bone should be made with caution.

Preliminary comparisons suggest the presence of taxon-specific inter-elemental variation of surface textures. Provided that this variation represents differential sequence of the relative timing of maturity among long bones, the nature of the variation could be correlated to differences in limb proportions and/or ontogenetic strategies among various avian taxa. Comparative work among birds with various body sizes, limb proportions, life histories and phylogenetic positions is needed to evaluate the significance of the variation, as well as to establish reliable ageing criteria for bird fossils.

**Acknowledgements**

This study is largely based on graduate work by JW under the guidance of HM at the Department of Geology and Mineralogy, Kyoto University. Completion of the work is largely thanks to generous assistance and valuable discussions by the members of the department. Attendance at the 8th International Meeting of the Society of Avian Paleontology and Evolution by JW was supported by an "Accommodation Grant" by the organizing committee of the meeting. Sincere gratitude is expressed to U. Göhlich (Naturhistorisches Museum Wien) for kind editorial support, and A. Tumarkin-Deratzian (Temple University, Philadelphia) and K. Campbell (Natural History Museum of Los Angeles County) for constructive comments on the manuscript that greatly improved the manuscript.

**References**

Baumel, J.J. & Witmer, L.M. (1993): Osteologia. – In: Baumel, J.J., King, A.S., Breazile, J.E., Evans, H.E. & vanden Berge, J.C. (eds.): Handbook of Avian Anatomy: Nomina Anatomica Avium. Second Edition. – *Nuttall Ornithological Club Publications*, **23**: 45–132.

Beale, G. (1985): A radiological study of the kiwi (*Apteryx australis mantelli*). – *Journal of the Royal Society of New Zealand*, **15**/2: 187–200.

Beale, G. (1991): The maturation of the skeleton of a kiwi (*Apteryx australis mantelli*) – a ten year radiological study. – *Journal of the Royal Society of New Zealand*, **21**/2: 219–220.

Bellaris, A. d'A. & Jenkin, C.R. (1960): The skeleton of birds. – In: Marshall, A.J. (ed.): Biology and Comparative Physiology of Birds, volume 1. – pp. 241–300, New York (Academic Press).

Bjordal, H. (1987): Metrical and mechanical properties of some skeletal bones from the House Sparrow, *Passer domesticus*, a contribution to the understanding of zooarchaeological problems. – *Ossa*, **13**/3: 49–59.

Boev, Z.N. (1987): [Morphometric features of the sexual dimorphism and individual variability of herons (Aves, Ardeidae) from Bulgaria II. Osteometric features.] – *Acta Zoologica Bulgarica*, **34**: 53–67. [in Bulgarian with Russian and English summaries]

Bourdon, E., Castanet, J., de Ricqlès, A., Scofield, P., Tennyson, A., Lamrous, H. & Cubo, J. (2009): Bone growth marks reveal protracted growth in New Zealand kiwi (Aves, Apterygidae). – *Biology Letters*, **5**/5: 639–642.

Bowler, J. (2005): Breeding strategies and biology. – In: Kear, J. (ed.): Ducks, Geese and Swans. Bird Families of the World, **16**. – pp. 68–111, Oxford (Oxford University Press).

Callison, G. & Quimby, H.M. (1984): Tiny dinosaurs: are they fully grown? – *Journal of Vertebrate Paleontology*, **3**/4: 200–209.

Cane, W.P. (1993): The ontogeny of the postcranial integration in the common tern, *Sterna hirundo*. – *Evolution*, **47**/4: 1138–1151.

Carrier, D.R. & Auriemma, J. (1992): A developmental constraint on the fledging time of birds. – *Biological Journal of the Linnean Society*, **47**/1: 61–77.

Carrier, D. & Leon, L.R. (1990): Skeletal growth and function in the California gull (*Larus californicus*). – *Journal of Zoology, London*, **222**/3: 375–389.

Carter, D.R., Mikić, B. & Padian, K. (1998): Epigenetic mechanical factors in the evolution of long bone epiphyses. – *Zoological Journal of the Linnean Society*, **123**/2: 163–178.

Chinsamy-Turan, A. (2005): The Microstructure of Dinosaur Bone: Deciphering Biology with Fine-Scale Techniques. – xii+195 pp. Baltimore (Johns Hopkins University Press).

Clark, A.H. (1907): Eighteen new species and one new genus of birds from eastern Asia and the Aletian Islands. – *Proceedings of the United States National Museum*, **32**/1539: 477–475.

Dial, T.R. & Carrier, D.R. (2012): Precocial hindlimbs and altricial forelimbs: partitioning ontogenetic strategies in Mallard duck (*Anas platyrhynchos*). – *Journal of Experimental Biology*, **215**/21: 3703–3710.

Fujioka, T. (1955): [Time and order of appearance of ossification centers in the chicken skeleton.] – *Acta Anatomica Nipponica*, **30**/2: 140–150. [in Japanese with English summary]

Haines, R.W. (1942): The evolution of epiphyses and of endochondral bone. – *Biological Reviews*, **17**/4: 267–292.

Hall, B.K. (2005): Bones and Cartilage: Developmental and Evolutionary Skeletal Biology. – xxviii+760 pp. San Diego (Elsevier Academic Press).

Hayward, J.L., Henson, S.M., Banks, J.C. & Lyn, S.L. (2009): Mathematical modeling of appendicular bone growth in glaucous-winged gulls. – *Journal of Morphology*, **270**/1: 70–82.

Hogg, D.A. (1980): A re-investigation of the centres of ossification in the avian skeleton at and after hatching. – *Journal of Anatomy*, **130**/4: 725–743.

Hogg, D.A. (1982): Fusions occurring in the postcranial skeleton of the domestic fowl. – *Journal of Anatomy*, **135**/3: 501–512.

Hohtola, E. & Visser, G.H. (1998): Development of locomotion and endothermy in altricial and precocial birds. – In: Starck, J.M. & Ricklefs, R.E. (eds.): Avian Growth and Development: Evolution within the Altricial-Precocial Spectrum. Oxford Ornithology Series, **8**. – pp. 157–173, Oxford (Oxford University Press).

Howard, H. (1929): The avifauna of Emeryville Shellmound. – *University of California Publications in Zoology*, **32**/2: 301–394.

Huggins, R.A., Huggins, S.E., Hellwig, I.H. & Deutschlander, G. (1942): Ossification in the nestling House Wren. – *Auk*, **59**/4: 532–543.

Klíma, M. (1965): Evaluation of the so-called skeleton sum method, employed in investigations on growth allometry in birds. – *Zeitschrift für Morphologie der Tiere*, **55**/3: 250–258.

Kushlan, J.A. & Hancock, J.A. (2005): Herons. Bird Families of the World, **14**. – xv+433 pp. Oxford (Oxford University Press).

Latimer, H.B. (1927): Postnatal growth of the chicken skeleton. – *American Journal of Anatomy*, **40**/1: 1–57.

Linnaeus, C. (1758): Systema naturae per regna tria naturae, secundum classes, ordines, genera, species, cum characteribus differentiis, synonymis, locis, I, 824pp. Stockholm (Laurentii Salvii).

Livezey, B.C. & Zusi, R.J. (2006): Higher-order phylogeny of modern birds (Theropoda, Aves: Neornithes) based on comparative anatomy: I. – Methods and characters. – *Bulletin of the Carnegie Museum of Natural History*, **37**: 1–544.

de Margerie, E., Robin, J.-P., Verrier, D., Cubo, J., Groscolas, R. & Castanet, J. (2004): Assessing a relationship between bone microstructure and growth rate: a fluorescent labelling study in the king penguin chick (*Aptenodytes patagonicus*). – *Journal of Experimental Biology*, **207**/5: 869–879.

Marples, B.J. (1930): The proportion of birds' wings and their changes during development. – *Proceedings of the Zoological Society of London*, **100**/4: 997–1008.

Milstein, P.S., Prestt, I. & Bell, A.A. (1970): The breeding cycle of the Grey Heron. – *Ardea*, **58**: 171–257.

Padian, K., de Ricqlès, A.J. & Horner, J.R. (2001): Dinosaurian growth rates and bird origins. – *Nature*, **412**/6845: 405–408.

Picasso, M.B.J. (2012): Postnatal ontogeny of the locomotor skeleton of a cursorial bird: greater rhea. – *Journal of Zoology*, **286**/4: 303–311.

Rogulska, T. (1962): Differences in the process of ossification during the embryonic development of the chick (*Gallus domesticus* L.), rook (*Corvus frugilegus* L.) and black-headed gull (*Larus ridibundus* L.). – *Zoologica Poloniae*, **12**/2: 223–233.

Sanz, J.L., Chiappe, L.M., Pérez-Moreno, B.P., Moratalla, J.J., Hernández-Carrasquilla, F., Buscalioni, A.D., Ortega, F., Poyato-Ariza, F.J., Rasskin-Gutman, D. & Martínez-Delclòs, X. (1997): A nestling bird from the Lower Cretaceous of Spain: implications for avian skull and neck evolution. – *Science*, **276**/5318: 1543–1546.

Serjeantson, D. (1998): Birds: a seasonal resource. – *Environmental Archaeology*, **3**: 23–33.

Serjeantson, D. (2002): Goose husbandry in Medieval England, and the problem of ageing goose bones. – *Acta Zoologica Cracoviensia*, **45**/special issue: 39–54.

Seymour, R.S., Smith, S.L., White, C.R., Henderson, D.M. & Schwarz-Wings, D. (2012): Blood flow to long bones indicates activity metabolism in mammals, reptiles and dinosaurs. – *Proceedings of the Royal Society, B: Biological Sciences*, **279**/1728: 451–456.

Starck, J.M. (1993): Evolution of avian ontogenies. – In: Power, D.M. (ed.): Current Ornithology, Volume 10. – pp. 275–366, New York (Plenum Press).

Starck, J.M. (1994): Quantitative design of the skeleton in bird hatchlings: does tissue compartmentalization limit posthatching growth rates? – *Journal of Morphology*, **222**/2: 113–131.

Starck, J.M. (1996): Comparative morphology and cytokinetics of skeletal growth in hatchlings of altricial and precocial birds. – *Zoologischer Anzeiger*, **235**: 53–75.

Starck, J.M. & Chinsamy, A. (2002): Bone microstructure and developmental plasticity in birds and other dinosaurs. – *Journal of Morphology*, **254**/3: 232–246.

Starck, J.M. & Ricklefs, R.E. (1998): Patterns of development: the altricial-precocial spectrum. – In: Starck, J.M. & Ricklefs, R.E. (eds.): Avian Growth and Development: Evolution within the Altricial-Precocial Spectrum. Oxford Ornithology Series, **8**. – pp. 3–30, Oxford (Oxford University Press).

Tumarkin-Deratzian, A.R., Vann, D.R. & Dodson, P. (2006): Bone surface texture as an ontogenetic indicator in long bones of the Canada goose *Branta canadensis* (Anseriformes: Anatidae). – *Zoological Journal of the Linnean Society*, **148**/2: 133–168.

Tumarkin-Deratzian, A.R., Vann, D.R. & Dodson, P. (2007): Growth and textural ageing in long bones of the American alligator *Alligator mississippiensis* (Crocodylia: Alligatoridae). – *Zoological Journal of the Linnean Society*, **150**/1: 1–39.

Turvey, S.T., Green, O.R. & Holdaway, R.N. (2005): Cortical growth marks reveal extended juvenile development of New Zealand moa. – *Nature*, **435**/7044: 940–943.

Turvey, S.T. & Holdaway, R.N. (2005): Postnatal ontogeny, population structure, and extinction of the giant moa *Dinornis*. – *Journal of Morphology*, **265**/1: 70–86.

Wolbach, S.B. & Hegsted, D.M. (1952): Endochondral bone growth in the chick. – *A.M.A. Archives of Pathology*, **54**/1: 1–12.

Yamashina, Y. (1941): A Natural History of Japanese Birds, volume 2. – 1080 pp. Tokyo (Iwanami Shoten). [in Japanese]